Faraday Discussions

Spiers Memorial Lecture: theory of unimolecular reactions

Journal:	*Faraday Discussions*
Manuscript ID	FD-ART-06-2022-000125
Article Type:	Paper
Date Submitted by the Author:	05-Jun-2022
Complete List of Authors:	Klippenstein, Stephen; Argonne National Laboratory, Chemical Sciences and Engineering Division

Spiers Memorial Lecture: theory of unimolecular reactions

Stephen J. Klippenstein

Chemical Sciences and Engineering Division, Argonne National Laboratory, Lemont, IL, 60439, USA

Abstract

One hundred years ago, at an earlier Faraday Discussion meeting, Lindemann presented a mechanism that provides the foundation for contemplating the pressure dependence of unimolecular reactions. Since that time, our ability to model and predict the kinetics of such reactions has grown in leaps and bounds through the synergy of ever more sophisticated experimental studies with increasingly high level theoretical analyses. This review begins with a brief historical overview of the progress from the Lindemann mechanism to the master equation, which now provides the cornerstone for most theoretical analyses. The current status of ab initio transition state theory based implementations of the master equation is then reviewed, beginning with a discussion of the energy resolved chemical conversion rates, followed by a review of the pressure dependence of the thermal kinetics. The latter discussion focusses on the collisional energy and angular momentum transfer rates as well as the complexities of non-thermal effects and of multi-well multiple channel reactions. The synergy with recent state-of-the-art experiments is used to motivate these discussions. Attempts to automate the calculations are also briefly reviewed. Throughout the discussion, we provide our perspective on current understanding and continuing challenges and opportunities. One key challenge relates to the coupling of sequences of reactions, which frequently leads to deviations from the classic presumption of thermal reactants.

1. Historical Overview

The year 2022 is a special time in the history of unimolecular reactions with many major milestones occurring. Most notably, this year marks the 100th anniversary of the Lindemann mechanism,[1] which remarkably still provides an effective framework for interpreting the kinetics of unimolecular reactions. Meanwhile, Rudy Marcus, the key figure in RRKM theory, [2] another major landmark for theoretical treatments of unimolecular reactions, celebrates his 100th birthday in 2023. Sadly, two other giants in unimolecular reaction theory, Bill Hase (who was noted for his analyses of non-statistical effects) and Jim Miller (who was noted for his applications of unimolecular rate theory to combustion kinetics as well as his work on the multiple well master equation), passed away in 2020 and 2021, respectively. I had the great fortune of extended close scientific and personal interactions with each of the latter 3 scientists. Indeed, as my Ph. D. advisor, Marcus was instrumental in formulating my perspective of what good science is. Meanwhile, Hase was one of the first scientists to appreciate my own independent efforts. My interactions with Miller began during the prime of my career. Our daily discussions during my time at Sandia (2000-2005) usually began with some review of a family or sports event, but generally led to some deep discussion on scientific matters. His profound insights into kinetics were a key driving force behind our collaborative efforts to advance the utility of the master equation as a tool for studying unimolecular reaction kinetics.

The Lindemann mechanism for "unimolecular" dissociation involves a two step process; excitation of a molecule A to an excited state A* via collisions with a bath gas M (together with the reverse deexcitation), followed by unimolecular decay of that excited molecule to products.

$$A + M = A^* + M \qquad (k_1/k_{-1}) \qquad (1)$$

$$A^* \rightarrow P \qquad (k_{diss}) \qquad (2)$$

Assuming a steady state of A* molecules yields,

$$d[P]/dt = k^{Lindemann}_{uni}\,[A] \qquad (3)$$

where

$$k^{Lindemann}_{uni} = k_1\, k_{diss}[M] / (k_{-1}[M] + k_{diss}) \qquad (4)$$

Notably, the Lindeman mechanism provides a rate that is linearly dependent on pressure, *P*, in the low-*P* limit and independent of *P* in the high-*P* limit. These limits are now accepted as generally correct, although radiative stabilization, tunneling, and pre-reactive complexes each affect these limits. Furthermore, the linear low-*P* limit is not generally applicable to the higher energy channel in reactions with multiple channels.

Although the Lindemann limits have the correct *P* dependence, the initial procedures for evaluating their prefactors were flawed. Key advances from the Lindemann mechanism initially arose from the incorporation of more details and improved expressions for the

excitation/deexcitation rates, and with explicit prescriptions for calculating the dissociation rate constant.[3] Most recently, the direct evaluation of each of the underlying theoretical parameters with ab initio electronic structure theory has allowed for deeper validation of the formalisms. Substantive comparisons between theory and experiment have been the driving force behind many of these developments.

A more physically correct treatment of the unimolecular dissociation process should account for the conservation of the total internal energy E and total angular momentum J of the molecules between collisions. This understanding, coupled with the use of quantum statistical theory expressions to compute both the dissociation rates and the collisional excitation rates (which are now E and J dependent) led to what has become known as RRKM theory.[2] An excellent overview of the sequence of efforts leading to the RRKM result is provided in the book of Holbrook et al.[3] For conciseness, we simply review the end result.

Within RRKM theory the single excitation/deexcitation process is replaced with a set of E and J dependent processes, thereby allowing for the proper inclusion of E and J resolved dissociation rate constants. Steady state approximations for each of the [A*(E,J)] then yields a temperature T and [M] dependent effective rate constant given by

$$k^{\mathrm{RRKM}}{}_{\mathrm{uni}}(T, [\mathrm{M}]) = \int dE\, dJ\, k_{\mathrm{diss}}(E,J)\, P(E,J)\, P_{stab}(E,J)\ , \qquad (5)$$

where $P(E,J)$ is taken to be the Boltzmann probability for a given E,J state, $\rho(E,J)\exp(-\beta E)/Q_{\mathrm{A}}$, with ρ as the density of electronic and rovibrational states of the reactant A, and Q_{A} the canonical partition function for A. The quantity β is simply $1/(k_{\mathrm{B}}T)$ where k_{B} is Boltzmann's constant and T is the temperature. The quantity P_{stab} denotes the stabilization probability for a molecule excited to an (E,J) state.

Within RRKM theory[2] the stabilization probability is simply taken as the probability that a collision with the bath gas occurs before the molecules dissociates:

$$\mathrm{P}_{\mathrm{stab}}(\mathrm{E,J}) = k_{\mathrm{c}}\,[\mathrm{M}]\,/[k_{\mathrm{c}}\,[\mathrm{M}] + k_{\mathrm{diss}}(E,J)] \qquad (6)$$

where k_{c} is the collision rate. Meanwhile, with transition state theory assumptions, the E,J-resolved dissociation rate may be written

$$k_{\mathrm{diss}}(\mathrm{E,J}) = \mathrm{N}^{\ddagger}(\mathrm{E,J}) / [\ h\, \rho(E,J)\ ] \qquad (7)$$

where the quantity $N^{\ddagger}(E,J)$ denotes the number of accessible states on the transition state dividing surface with an energy less than or equal to E and in angular momentum state J. The J dependence of the rate constant is often ignored.

The transition state is a key concept in unimolecular rate theory. It is an N-1 dimensional hypersurface (where N is the number of degrees of freedom in the system) that is presumed to completely separate reactant and product regions of phase space. In particular, every trajectory that passes through the dividing surface is presumed to proceed directly on to products without ever recrossing the dividing surface. When the "true" transition state dividing surface is replaced

with an approximate physical realization of it, as in essentially all numerical implementations of transition state theory (TST), the resulting rate overestimates the true rate for a statistical distribution of initial states. Correspondingly, variational minimization of the transition state dividing surface within some family of representations provides an improved estimate of the statistical dissociation rate. Numerical implementations of this variational principle play an important role in high accuracy TST based predictions.[4] Because E and J are strictly conserved between collisions, it is most accurately implemented at the E,J-resolved level, with appropriate thermal averaging. Commonly though, it is instead implemented at the canonical level, which yields modest overpredictions (e.g., 20%) in the rates.

A key aspect of RRKM theory is that it provides explicit statistical theory based prescriptions for the evaluation of it parameters. Early on, experimental work by Rabinovitch and coworkers was instrumental in demonstrating the basic validity and utility of the RRKM formalism.[5] Subsequent comparisons were ever more stringent, as progress was made in first principles procedures for evaluating the components of RRKM theory, and as more and more sophisticated experimental probes were designed. In this review, we consider some very recent tests of the RRKM expression for the E/J resolved dissociation rate, Eq. (7).

Notably, the RRKM form retains the two key results from the Lindemann mechanism: linear in P at low-P, and independent of P in the high-P limit. However, it does show a stronger deviation from those two limits at intermediate pressures (i.e., in the falloff regime). Accurately treating that deviation is a key focus of improving the theoretical description. One clear shortcoming in the RRKM derivation is the assumption that every collision is fully stabilizing. Simple attempts at improving RRKM theory replace the collision frequency k_c in Eq. (6) with β_c k_c, where β_c is some number less than unity, to obtain a modified strong collider version of RRKM theory. In essence, the factor $1/\beta_c$ is meant to correspond at least qualitatively to the number of collisions required for stabilization of the excited state populations.

Substantive improvements to RRKM theory arise from quantitative treatments of the collision induced flow of energy, particularly for states that lie in the neighborhood (within about 10 k_BT) of the dissociation threshold. The "one-dimensional" master equation (1DME) represents the time dependence of the full set of E-resolved state populations in terms of the rates for collision induced transitions in molecular rovibrational states and E-resolved dissociation rates. In the "two-dimensional" master equation (2DME) one also considers the collision induced transitions in J (cf. Fig. 1) and the dissociation rate is evaluated at the E,J-resolved level. For a simple single well,

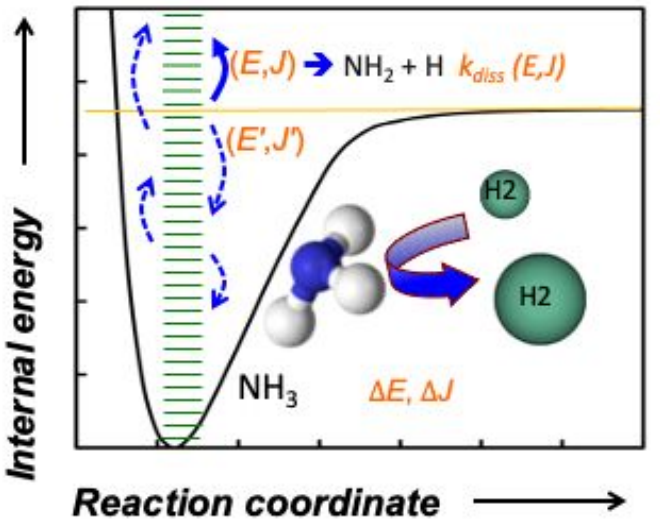

Fig 1: Schematic diagram of the collision induced dissociation process for ammonia decomposition.

single channel dissociation the lowest eigenvalue of the master equation is directly related to the *T* and *P* dependent dissociation rate.[3,6]

As illustrated in Fig. 2 for a representative calculation of the dissociation of formaldehyde ($H_2CO \rightarrow H_2 + CO$), the 1DME again yields a rate constant that shows linear in *P* behavior in the low-pressure limit and approaches a constant value at high pressure. However, the Lindemann and RRKM models fail to capture the full extent of the "falloff" in the rate constant for intermediate pressures. For the illustrative purposes of this calculation, neither tunneling or radiative emission effects are included. Those effects will instead be discussed later as part of the main review.

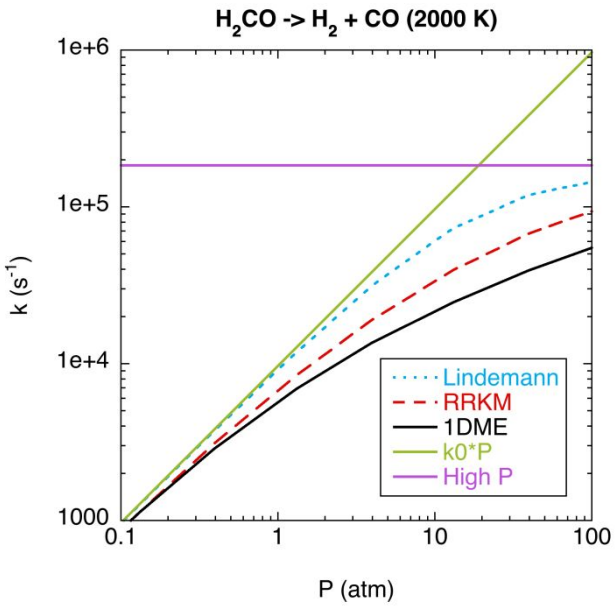

Fig. 2: Plot of $k(P)$ at T=2000 K for formaldehyde dissociation for various models. Note the calculations do not include tunneling or radiative emission.

Troe was instrumental in demonstrating the utility of the one channel 1DME approach.[7,8] His simplified expressions connecting the master equation solutions to molecular properties have provided the basis for many an application of unimolecular reaction rate theory.[9] Furthermore, his empirical expressions for representing the *T* and *P* dependence of the master equation solutions have become the de facto standard for combustion modeling.

When I moved to Sandia to work on combustion kinetics with Jim Miller, one of the problems that he really wanted to solve was the treatment of complex multiple well, multiple channel reactions. This interest was driven by a desire to properly model the reaction of C_3H_3 + C_3H_3, which he considered to be the most important reaction in the formation of the first aromatic ring,[10] which in turn was deemed to be the most important step in first PAH (polycyclic aromatic hydrocarbon) and then soot formation. At the time, I had just collaborated with Struan Robertson in coupling his master equation methodologies with our variable reaction coordinate transition state theory methodologies[11] within the VariFlex code.[12] To satisfy Jim's interests I first took on the task of extending the VariFlex code to multiple-well multiple-channel (MWMC) reactions. Fortunately for me, Struan generously shared some of his own MWMC master equation codes,[13] which greatly simplified the task.[14]

For kinetic modeling purposes, the time dependent solutions to the master equation still needed to be connected to the phenomenological rate constants describing the time dependence of the species concentrations. Initially, we followed an "experimentalist's" approach, where we tried to find initial conditions for which the populations would decay exponentially and could thus be related to the rate constants. This approach was reasonably successful for systems that were not too complex. Indeed, it proved effective for comparing theory with the groundbreaking

experimental measurements of radical oxidation being performed in the Taatjes lab at the time.[15,16] However, when we tried to use this approach for the $C_3H_3 + C_3H_3$ reaction, we found the overlap in the decays to be much too complex to allow for a direct extraction of individual rate constants one at a time. I reluctantly gave up on that approach before too long.

It then occurred to me that there should be a one-to-one correspondence between the phenomenological rate coefficients and the eigenvalues and eigenvectors describing the chemical transformations (as opposed to the internal energy relaxation arising from the collision energy transfer process). With this recognition it was then straightforward to analytically connect the phenomenological rate coefficients to the eigensolutions of the master equation by simply considering the time dependence of the solutions after the fastest, non-chemical, contributions had decayed away.[17] Jim then took the task of elegantly expanding my derivations[17-19] and in the process recognized a connection to some earlier, underappreciated work of Bartis and Widom.[20] With this approach in hand, we could finally tackle the $C_3H_3 + C_3H_3$ reaction, which led to quantitative explanations for a number of existing observations.[21] We also made generic predictions for the *T* and *P* dependence of the full set of phenomenological rate coefficients, some of which were subsequently validated experimentally.

Interestingly, as part of this discussion meeting, some aspects of the isomerizations on the $C_3H_3 + C_3H_3$ potential energy surface (PES) were revisited by Osborn and coworkers with threshold photoelectron photoion coincidence (PEPICO) spectroscopy.[22] The PEPICO technique is also used by Hochlaf and coworkers to examine the fs timescale dissociation dynamics of neutral and ionic pyruvic acid.[23] In a follow up study of the $C_3H_3 + C_3H_3$ reaction, we replaced our initial empirical PES model based variable reaction coordinate (VRC)-TST approach for the "barrierless" entrance channel kinetics, with a direct CASPT2 based VRC-TST analysis.[24] The VRC-TST approach provides a quantitative treatment of the interfragment mode couplings including a full analysis of their anharmonicities.[11] The statistical adiabatic channel model, which provides an alternative to VRC-TST, is applied by Troe and coworkers to the N + OH reaction in a paper presented at this meeting.[25]

There are now a number of fairly well developed freeware master equation codes for treating MWMC reactions that are receiving wide spread use. These include the MESMER[26,27] and TUMME[28,29] codes from the Robertson and Truhlar teams, respectively, as well as the MESS code from Georgievskii.[30,31] These codes rely on the chemically significant eigenvalue (CSE) approach for connecting the master equation to the phenomenological rate coefficients,[17-19] while the MultiWell code of Barker and coworkers[32,33] instead relies on a stochastic approach with numerical fitting of the rates. Both the large span of eigenvalues and the merging of chemical and energy relaxation eigenvalues occasionally limit the range of applicability of the CSE approach. Efforts to improve the numerical stability and range of applicability of the solutions continue, as discussed further below, as well as in the paper of Johnson and Green from this meeting.[34]

The above-described advances in the theoretical framework for treating the kinetics of unimolecular dissociation have been followed by ever more sophisticated numerical implementations of the framework. These numerical implementations rely on methodologies for predicting partition functions (canonical and microcanonical), collisional energy transfer kernels (with and without *J* resolution), barrier heights, tunneling probabilities, and nonadiabatic transition

rates. Of course, the progress in electronic structure theory from an empirical science to a highly predictive one has been at the heart of these advances. Currently, each of these quantities may now generally be predicted to a high degree of accuracy with first principles theoretical methodology. As a result, comparisons between state-of-the-art numerical implementations of the "ab initio transition theory based master equation" (AI-TST-ME) approach with experiment now provide definitive tests of the theoretical framework.

These advances in our theoretical understanding have been driven by the desire to (i) better understand and model ever more sophisticated, detailed, and wide-ranging experimental observations and (ii) build high fidelity chemical mechanisms for complex chemically reactive mixtures. Recent years have seen exquisitely detailed and precise observations of energy resolved dissociation rate constants, as well as measurements of thermal rate constants, branching ratios, and time dependent species populations covering vast ranges of temperature (from a few K to more than 2000 K) and pressure. Furthermore, novel methods for observing some of the most ephemeral chemical species provide further challenges and tests for the theoretical methodologies. Notably, more global experimental observations of the evolving species concentrations in complex chemically reactive environments are now driving improved understanding of the connection between sequences of unimolecular and bimolecular reactions. It is now clear that the classic model of separated sequences of reactions between thermally equilibrated clearly is not generally correct. With the current state of theory, an important new driving force is a burgeoning desire to develop fully first principles based theoretical models for the whole complex chemically reactive environments.

This review begins with a discussion of energy resolved chemical conversion rates. First a recent experimental study of a QOOH (hydroperoxyalkyl radical) dissociation is used to motivate a review of the advances in theoretical methodologies for predicting $k(E)$. Then related studies of Criegee intermediates are used to motivate discussions of the chemical complexities that can arise in unimolecular dissociations. After that, we proceed to discuss the pressure dependence of unimolecular dissociation kinetics. This discussion ranges from collisional E and J transfer calculations to the MWMC master equation. Summary of the numerical implementations, comparisons with experiment, and remaining challenges are included throughout. We should perhaps note that this review is not meant to be exhaustive, but rather to simply touch on some interesting aspects of unimolecular reactions that are of current topical interest.

2. Chemical Conversions and RRKM Theory

Energy resolved observations of the dissociation process provide valuable tests of theoretical models for the chemical aspects of the dissociation process. Early observations of energy dependent dissociation rates for cycloheptatrienes,[35] NCNO,[36,37] CH_2CO,[38-43] H_2CO,[44] NO_2[45-47] and hydroperoxides,[48] provided valuable tests of the RRKM model for the E and/or E,J-resolved collision-free dissociation process [Eq. (7)]. The generally good agreement between RRKM models and experimental measurements provided strong conformation of the general validity of the statistical and transition state theory assumptions underlying the RRKM expression.

Related observations for ionic compounds led to similar conclusions.[49,50] For ionic molecules, confidence in the RRKM models grew to the extent that the community has long used

them as key components of procedures for determining binding energies.[51-53] A new application of RRKM-based modeling to radical ion + molecules by Trevitt and coworkers in this discussion meeting finds good agreement with companion experimental observations.[54] The dissociation dynamics of multiply-charged ions are of increasing interest as an analytic tool. A paper in this discussion by Vallance and coworkers illustrates the use of covariance-map imaging to explore the plausible dissociation mechanisms.[55]

In recent years, the Lester group has developed a novel and very effective methodology for examining the *E,J*-resolved dissociation of highly unstable reactive intermediates.[56,57] Their approach involves an in situ generation of the intermediate coupled with stabilization in a pulsed jet expansion followed by time-resolved IR pump-UV probe action spectroscopy. Variation of the IR pump wavelength yields *E*-resolved dissociation rate constants for a variety of energies. The UV probe is used to observe laser-induced fluorescence of OH radicals. These new observations from the Lester group provide important new challenges and tests for theoretical models. Thus, we will use them as a focus for our discussion.

2.1 QOOH Decomposition Kinetics

Chain branching in low temperature oxidation is a key feature of atmospheric and combustion chemistry. This chain branching arises from a sequence of two O_2 additions to a radical following by decomposition of the ketohydroperoxide product. Eskola and coworkers have recently presented theory-experiment studies of the thermal kinetics for the first stage of this process,[58] including for the pent-3-en-2-yl radical as part of this discussion meeting.[59] These studies illustrate the utility of automated parameter optimization within AI-TST-ME calculations. The addition of the second O_2 is preceded by an internal H migration to form a carbon centered QOOH (hydroperoxyalkyl) radical.

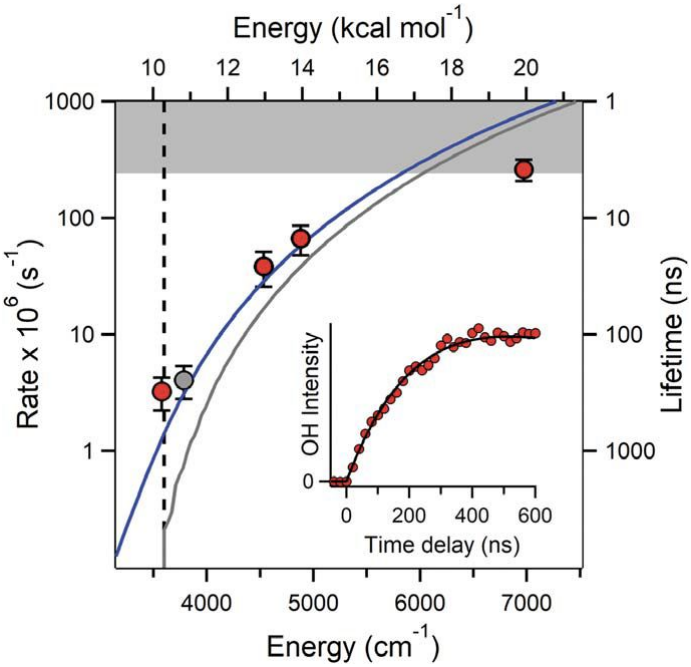

Fig. 3: Energy-dependent unimolecular decay rates for the decomposition of $CH_2C(CH_3)_2OOH$. Experimental rates and corresponding lifetimes are denoted with symbols, with ±1σ error bars. The solid lines denote ab initio RRKM predictions with (blue) and without (gray) tunneling corrections. The vertical dashed lines denote the saddle point barrier of 10.3 kcal mol^{-1}. The inset shows a representative time trace for the appearance of OH products. From Ref. 60. Reprinted with permission from

Recently, the Lester group used their in situ synthesis plus time-resolved IR pump-UV probe action spectroscopy method to directly probe the dissociation of a prototypical QOOH radical, $CH_2(CH_3)_2COOH$.[60] These radicals are central to chain branching in low temperature oxidation, but there have been very few direct studies of their

kinetics due to their ephemeral nature. Their reaction with O_2 ultimately leads to the conversion of one radical into three. A quantitative understanding of the dissociation rate is of key importance because it occurs in direct competition with the reaction with O_2.

We collaborated with Lester in developing an AI-TST-ME model for the dissociation reaction, $CH_2(CH_3)_2COOH \rightarrow$ cyc-$CH_2OC(CH_3)_2$ + OH. As illustrated in Fig. 3, the theoretical predictions are in quantitative agreement with the experimental observations, with only a minor discrepancy occurring at the lowest energy, which lies slightly below the barrier threshold. The apparent discrepancy at the highest energy correlates with a limit in instrument resolution, as denoted by the gray shaded region. This agreement nicely validates RRKM theory for a very weakly bound molecule (barrier height of only 10.3 kcal mol^{-1}). It relies on the use of high accuracy methods for evaluating the tunneling probabilities, the barrier height, the density of reactant states, and the transition state number of states, as discussed below.

2.1.1 Tunneling

Our collaborative study of the QOOH decomposition highlights the importance of heavy atom tunneling. The reaction coordinate for this system involves a combination of OO stretching and OCC bending motions. The lower gray curve in the plot of Fig. 3 illustrates the predicted dissociation rate in the absence of tunneling. The tunneling effect at the lowest energy is about a factor of 5 and remains significant up to about 4 kcal mol^{-1} above the barrier top. As reported in a paper for this discussion meeting, Lester has followed up this work with a related study of the dissociation of a selectively deuterated form of the radical, QOOD, where the deuteration is of the OH group.[61] The agreement between related RRKM predictions for this isotopically substituted reaction, with nearly identical tunneling frequency, strongly validates the proposed significant role for heavy atom tunneling.

There are currently a variety of practical methods for predicting tunneling probabilities. The asymmetric Eckart model provides a particularly simple one-dimensional tunneling correction that is very widely used due to its simplicity.[62] Its implementation requires only the barrier height, reaction energy, and imaginary frequency for the reaction coordinate. However, it neglects multidimensional tunneling effects that can be quite important. The small and large curvature tunneling methods of Truhlar and coworkers[63-66] explicitly consider the multidimensional aspects of the tunneling process. These methods have also found widespread use, in part due to their effective direct dynamics implementation within the freeware PolyRate code,[67] as well as their sound theoretical basis. More recently, the semiclassical transition state theory (SC-TST) approach[68] has gained in popularity, in part because of the current facility of generating the requisite anharmonicity parameters with readily available electronic structure codes. Barker, Stanton, and their coworkers applied this approach to the OH + CO addition elimination reaction[69,70] as well as a number of abstraction reactions. For this discussion meeting, Stanton and coworkers apply SC-TST to an analysis of the H + C_2H_4 reaction system.[71] Meanwhile, Clary has explored the effectiveness of reduced dimensionality simplifications in the SC-TST approach that facilitate its widespread use for larger molecules.[72]

The SC-TST approach is based on perturbation theory and does not incorporate variational effects. As such, it might be expected to fail to some degree in both the low-temperature deep

tunneling regime, where the potentials deviate from their perturbative expansions,[73] and the high temperature regime, where variational effects become significantly. Notably, for many abstraction reactions, variational effects are quite significant even at 0 K because the zero-point corrected barrier is displaced by a large distance from the electronic barrier. More work is needed to compare the SC-TST approach to the variationally corrected reaction path approaches of Truhlar over broad ranges of temperature.

Our calculations for the QOOH decomposition[60] employed a new semiclassical tunneling approach derived by Georgievskii.[74] In this work, a closed-form rate expression was obtained that explicitly treats the nonseparability of tunneling from other vibrational coordinates. The expression was also extended to properly account for the conservation of angular momentum, although a numerical implementation of that has not yet been provided. For our QOOH study, we employed a perturbative form of this approach that bears some similarity to the SC-TST approach including its nonvariational nature, but also differs in significant ways, including the contribution of a novel term, which was labeled the entanglement factor. Its implementation is also more straightforward and requires less PES information than does SC-TST. Interestingly, the perturbative form of this approach provides a natural decomposition of the tunneling action into components from different vibrational modes and also explains in simple terms the quantum bobsled and MEP curvature effects. In future work, it will be interesting to explore the role of angular momentum on tunneling probabilities, which has largely been neglected in prior work and to numerically contrast this approach with SC-TST and the reaction path based approaches of Truhlar.

2.1.2 Electronic structure theory

For many years, the goal of electronic structure theory was to provide "chemically accurate" energies, which came to mean absolute errors of 1 kcal mol^{-1} or less. Ultimately, a variety of different approaches were found to yield this level of accuracy or better. Each of these approaches were in essence based on some form of approximation to the complete basis set (CBS) limit of the CCSD(T) (coupled cluster with singles doubles and perturbative triples) method. The popular G4[75] and CBS-QB3[76] methods achieve 2σ accuracies of 1.1 and 2.4 kcal mol^{-1}, respectively for a set of 114 combustion relevant heats of formation.[77] While methods with 1-2 kcal mol^{-1} accuracies have many utilities, they are not really effective for making first principles kinetics predictions, especially for atmospheric chemistry. For example, at room temperature the Boltzmann factors for 1 and 2 kcal mol^{-1} energies are 0.19 and 0.035, respectively.

The explicitly correlated CCSD(T)-F12 method dramatically improves the ability to approach the CCSD(T)/CBS limit.[78] Furthermore, domain based local correlation methods allow for the generation of approximate CCSD(T)/CBS limit energies for molecules with tens of heavy atoms, but at the cost of modest deviation from the true CCSD(T)/CBS limit. Effective implementations of the DLPNO-CCSD(T)[79,80] and the PNO-LCCSD(T)-F12[81] methods, are now available in the widely available Orca[82] and Molpro[83,84] software packages. Proper evaluation of the CCSD(T)/CBS limit should lead to reduced errors relative to composite methods such as G4 and CBS-QB3. However, the 2σ errors are unlikely to fall much below about 1.0 kcal mol^{-1}, due to limitations in the CCSD(T) method itself.

Major further reductions in the error of ab initio energy predictions have been obtained by a number of groups through the inclusion of a variety of corrections to the CCSD(T)/CBS limit as well as by better approaching that limit through the use of larger basis sets, with better geometry optimizations and frequency evaluations.[85-88] As shown in our recent wide ranging analysis of combustion enthalpies (cf. Fig. 4), the most important correction involves the CCSDT(Q) correction, while core-valence and anharmonicity corrections are also quite significant. [77] Meanwhile, relativistic and Born-Oppenheimer corrections are typically quite small.[77] Substantive comparisons of our ANL methods[77] with reference values from the active thermochemical tables approach[89-91] indicate 2σ errors of 0.2 kcal mol^{-1}, as long as the CCSDT(Q) correction is not too large. Large CCSDT(Q) corrections are indicative of significant multi-reference effects, for which alternative multireference approaches should be used. Notably, a room temperature Boltzmann factor for an uncertainty of 0.2 kcal mol^{-1} is 0.72, at which point the accuracy of kinetic theory is starting to rival that of many experiments.

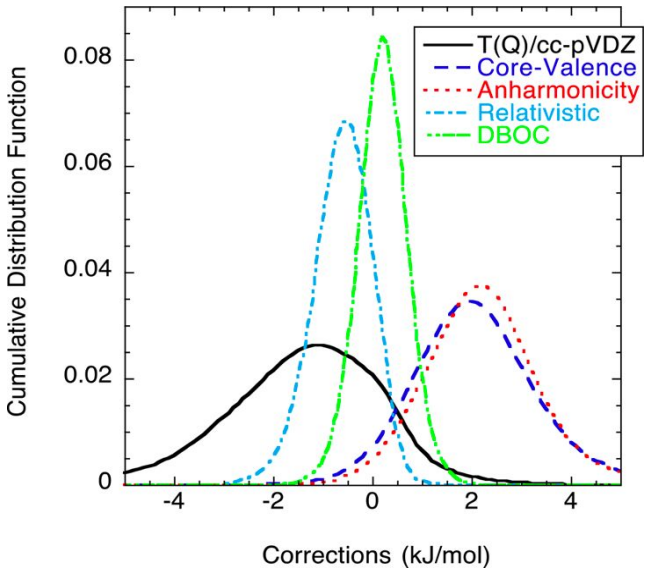

Fig. 4: Plot of the cumulative distribution function for the ANL0 corrections for higher order excitations [CCSDT(Q)/DZ], core-valence interactions, vibrational anharmonicity, relativistic, and Born-Oppenheimer effects. Reprinted with permission from Ref. 77. Copyright 2017 American Chemical Society.

The need for accurate geometries and zero-point energies is often underappreciated. Doubly hybrid density functional methods provide geometries and harmonic zero-point energies for minima that rival the accuracy of CCSD(T) values. We have found the B2PLYP functional[92] with a cc-pVTZ basis set to be very effective in that regard, while the newly optimized revDSD-PBEP86-D3BJ functional appears to provide slightly higher accuracy at similar cost.[93] Unfortunately, for transition states there are still significant errors in such DFT geometries – at least there are often significant discrepancies in the geometries obtained at the CCSD(T) and B2PLYP or revDSD levels. For coupled cluster methods, it important to use a large enough basis set in such determinations. Currently, we prefer to use CCSD(T)-F12 based saddle point geometries and harmonic frequencies, as the most reliable yet feasible approach at our disposal. For our study of the QOOH decomposition we found that CCSD(T)-F12/cc-pVDZ-F12 geometry and frequency optimizations were an essential part of achieving a high accuracy barrier height. The remaining components of the barrier height were obtained according to the ANL0-F12 methodology, except for the CCSDT(Q) correction, where a smaller 6-31G* basis was used in place of the cc-pVDZ basis.[60]

It is important to also consider the effect of vibrational anharmonicities on the zero-point energy. Second order vibrational perturbation theory (VPT2) provides a straightforward procedure for doing so.[94] Density functional and coupled clustered implementations generally yield quite

similar anharmonic ZPE corrections. However, the VPT2 procedure itself occasionally fails, particularly for low frequency torsional and umbrella motions. Harding and coworkers have demonstrated the utility of diffusion Monte Carlo calculations for such problematic cases.[95]

We have observed irregularities in such VPT2 calculations for abstraction reactions. For example, in the $OH + H_2 \rightarrow H_2O + H$ reaction at the CCSD(T)/cc-pVQZ level, the second highest harmonic frequency is at 2591 cm^{-1}, while the corresponding anharmonic fundamental is at 3747 cm^{-1}. Such large anharmonic corrections have significant ramifications for rate predictions. Notably, the calculated anharmonic values are remarkably sensitive to method. For example, at the B2PLYPD3/cc-pVTZ and B3LYP/cc-pVTZ levels the anharmonic values for this mode are instead 4190 and 4629 cm^{-1}, respectively. This behavior appears to be related to a strong coupling of the symmetric and asymmetric stretching coordinates. The method dependence then arises from the substantially different lengths for the forming OH bond in the TS: 1.346, 1.373, and 1.412 Å for the CCSD(T)/cc-pVQZ, B2PLYPD3/cc-pVTZ, and B3LYP/cc-pVTZ methods, respectively. This issue is quite common in OH abstraction reactions and deserves further study.

A number of recently presented methods such as the W3X-L,[96] diet-HEAT-F12,[97] and mHEAT[98] methods bear many similarities to the ANL0 and ANL0-F12 methods. These methods were designed to reduce the cost of the original W4 and HEAT methods by constraining the most expensive parts of the composite scheme, while retaining some form of CCSDT(Q) correction, much as was done with the ANL methods. The most expensive part of these calculations, as well as the part that effectively determines the accuracy, is the CCSDT(Q) evaluation for a double-zeta quality basis set. This required CCSDT(Q) evaluation limits our use of the ANL0 methodology to systems with about 6 or fewer heavy atoms. Fortunately, prototypes for most classes of reaction can be captured with 6 heavy atom systems.

Various literature approaches attempt to obtain high accuracy at reasonable costs by building in some type of empirical correction or reference scheme. The recently developed WMS[99] composite approach of Truhlar and coworkers aims to reproduce the accuracy of the W3X-L method[96] at dramatically reduced cost (i.e., approximately that of the G4 method) through separate scalings of the individual terms. The incorporation of bond additivity corrections (BAC), as in the pioneering BAC-MP4 work of Melius,[100] can correct for many of the deficiencies in approximate quantum chemistry models. For example, a BAC-QCISD(T)/CBS analysis of Goldsmith et al.[101] yields 2σ uncertainties of about 0.5 kcal mol^{-1}.[77] Alternative procedures use chemically similar species as references (e.g., with isodesmic and related reactions[102]), which often allows for high accuracy predictions at relatively low levels of theory, as long as the references are accurately known. Such isodesmic schemes have found considerable utility in recent combustion studies (see, e.g., Ref. 103).

The connectivity-based hierarchy (CBH) scheme of Raghavachari and coworkers[104-106] provides a useful explicit prescription for systematically choosing larger and larger reference species that increasingly represent the chemical environment of the target molecule. We have implemented an automated version of the CBH schemes within our freeware automated kinetics software package AutoMech.[107-109] We find that the CBH-2 methodology coupled with ANL0 reference energies provides a very effective means for predicting enthalpies of formation. For example, sample B2PLYPD3/cc-pVTZ calculations with the ANL0-CBH-2 scheme for a set of

alkane oxidation related species yielded a maximum error of 0.7 kcal mol^{-1} relative to corresponding CCSD(T)-F12/cc-pVTZ-F12 ones (cf. Fig. 5).[109]

It should be possible to design and generate similarly effective post facto corrections for barrier height evaluations. For example, a study of Knyazev illustrates the utility of an isodesmic reaction type approach for energy barriers.[110] Meanwhile, a recent study of Karton provides high quality for data for a set of 28 reactions.[111] Overall, more effort is needed at designing well validated correction schemes for transition states. Of course, with sufficient high quality data, machine learning will become an effective tool for predicting barriers for larger sets of reactions.

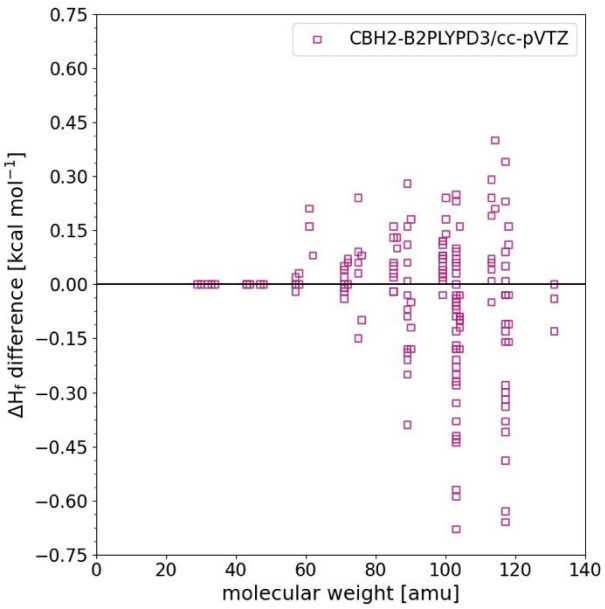

Fig. 5: Difference between B2PLYPD3/cc-pVTZ and F12-CCSD(T)/cc-pVTZ-F12 energies for a set of 150 RH, R, RO_2, and QOOH species Both calculations employed an ANL0 reference based CBH-2 scheme.[109]

2.1.3 Anharmonic State Counts

Rigid-rotor harmonic-oscillator models provide the foundation for most evaluations of the reactant and transition state partition functions and state densities. Nevertheless, it is well understood that various forms of anharmonicities can significantly affect the state counts. In particular, torsional modes of the molecules are not well represented as a harmonic oscillator, and some form of hindered rotor correction is generally employed. The umbrella/inversion mode in radicals is also often highly anharmonic, although this fact is often ignored. Furthermore, the umbrella and torsional modes are often strongly coupled, and limitations in the treatment of this coupling are perhaps the single biggest shortcoming in many calculations.

The partition functions for the remaining, higher frequency, vibrational modes generally show a few percent deviation from the harmonic limit for each mode, with this deviation increasing with temperature.[112] For larger molecules, the total number of vibrational modes results in a substantial total anharmonic effect (e.g., a 6 heavy atom molecule might have 50 vibrational modes yielding more than a factor of two effect on the partition function at 1000 K). For reaction rate calculations, the effects of the anharmonicity on the transition state and the reactant often, but not always, cancel out to a significant degree. For absolute thermodynamic properties, quantitative inclusion of anharmonicity corrections is essentially always required.

Jasper and coworkers recently employed Monte Carlo phase space integration to calculate the fully anharmonic partition functions for a large set of systems.[112,113] These calculations, which employed high quality PESs and included systems with up to three “fluxional” (torsions and umbrella inversions) modes and 30 degrees of freedom, provide valuable benchmarks for more approximate approaches. Simpler approaches generally employ some form of assumed separation between the fluxional and remaining higher frequency vibrations. The analysis of Jasper explored

the accuracy of such presumed separability approximations, as well as the appropriateness of decoupled one-dimensional treatments of the fluxional modes.

Within assumed separability approaches, the anharmonicities in the higher frequencies are often ignored, or else simply treated through the use of an estimated fundamental frequency within the RRHO expressions (e.g., from VPT2 or scaling relations). Such corrections seem reasonably accurate up to about 1000 K, but increasingly fail beyond that. It is perhaps worth noting that explicit state counting based on VPT2 expressions commonly leads to issues related to turnovers in the energy versus quantum number. These issues, which are simply indicative of the limits of a perturbation theory approach, tend to be particularly severe for transition states.

The most common approach for treating torsional anharmonicities involves a presumed separation into a set of decoupled one-dimensional hindered rotors (1DHR). This approach is often preferred, especially for larger systems, because the effort involved in the expansion of the potential is proportional to the product of the number of rotors (n_{rotor}) and the number of grid points per rotor (n^{grid}). In contrast, for grid based multidimensional hindered rotor (MDHR) analyses the computational effort is proportional to $(n_{grid})^{nrotor}$. Such MDHR analyses, which are available in some current software,[27,31,114] are reasonably effective for up to about 3 or 4 rotors. Of course, the decrease in cost for the 1DHR comes with a corresponding decrease in accuracy.

Although seldom discussed, there are important choices to make in implementing one-dimensional hindered rotor representations. For example, three simple alternatives may be used in performing the torsional scans: (i) all coordinates except for the torsion of interest may be optimized at each grid point, (ii) only the non-torsional degrees of freedom may be optimized, or (iii) all coordinates could be held fixed at the values of some reference geometry. There is also an important choice to be made in the reference conformer about which to perform the 1DHR scans. Commonly, the reference geometry is taken to be that with the lowest potential energy in some preliminary conformer sampling. However, the zero-point energy can vary quite substantially among conformers. In that case, one might expect the conformer with the lowest zero-point corrected energy to provide the best reference geometry since it would have the largest contribution to the zero K enthalpy. Generalizing that concept, one might instead choose a reference conformer that has the lowest Gibb's free energy at the temperatures of interest. The latter choices can be useful in avoiding hydrogen-bonded configurations that commonly have the lowest potential energy but do not contribute as much to the partition function at the higher temperatures of practical interest.

Ideally, one would like a 1D based approach to reproduce the harmonic oscillator limit at low temperature, and a free-rotor limit at higher temperatures. However, symmetry aspects of the torsional motions often imply that one would need to use temperature dependent symmetry numbers in order to achieve this. This difficulty arises because the product of 1DHRs often do not sample the full set of equivalent minima. The problem is exacerbated by the coupling of inversion and torsional motions. Indeed, it is often difficult to tell a priori if a 1D torsional mapping will find the full set of inversion and torsional minima or just a set of torsional minimum related to one fixed form of the inversion. Practically, we find that the preferred choice of symmetry number is most often the higher value that correlates with the value appropriate for a MDHR sampling.

For our study of the QOOH decomposition we employed multidimensional rotor representations.[60] In this case, one of the primary advantages of the MDHR approach was in its proper treatment of the symmetry aspects of the problem. In our study of the dissociation of methyl ethyl Criegee intermediate (MECI),[115] we compared the results of a MDHR approach with those from both RRHO and 1DHR based approaches. Here, some of the differences were more substantive. For both cases, we incorporated anharmonic effects for the higher frequency modes through the use of the VPT2 expressions for the fundamental frequencies.

An alternative approach to treating the rotamer aspects of the problem involves a representation of the partition function in terms of a sum of contributions from each of the conformational minima. The simplest form of multi-conformer approach employs a sum of RRHO expansions about the minima (see, e.g., Refs. 116, 117). This approach should be quite accurate at low enough temperatures (e.g., room temperature) and when only considering the high pressure limit. At higher temperatures, and for falloff where the density of states at the dissociation threshold is needed, the harmonic expansions can lead to an overcounting of the available phase space. For these reasons, Truhlar and coworkers developed an alternative form of multi-conformer transition state theory where they evaluate the contributions from each conformational minimum with local expansions that account for the full multidimensional nature of the problem.[118-120]

This multi-structural torsional (MS-Tor) approach of Truhlar and coworkers is highly effective, and widely used, but is limited to cases where all the minima can be mapped out. A recent study from Ren and coworkers explores a multistructural 2-dimensional torsion approach that extends the applicability of the MS-Tor approach to much larger molecules.[121] A recent study from Zhang and coworkers[122] suggests a Voronoi tessellation based procedure for correcting an apparent overestimate in the MS-AS (multi-structural all-structures) version[123] of the MS-Tor approach. Later versions of the MS-Tor approach[120] employ a coupled potential approximation that also appear to deal with the shortcoming addressed by Zhang and coworkers.

Unfortunately, most applications of the MS-Tor approach have focused on comparisons with simple single conformer RRHO results, which naturally indicate major anharmonicity effects. It is less clear how substantive the deviations generally are for a high quality 1DHR approach. Zhang and coworkers do indicate significant deviation from a 1DHR model for the reactions of HO_2 with methylbutanoate.[124] These reactions have a high degree of hydrogen bonding, which is likely the primary cause for these deviations. It would be interesting to compare these MS-Tor results with 1DHR calculations that employ the lowest Gibbs free energy conformer as a reference instead of the lowest energy conformer.

An alternative Monte Carlo integration based approach to evaluating the MDHR contributions[125] to the canonical partition function is incorporated in MESMER.[27] One appealing feature of this approach is its lack of any approximation in the hindered rotor mode couplings, at least for a given potential energy surface and within a classical framework. Note that the canonical partition functions are readily converted to microcanonical state densities within MESMER via invert Laplace transform, which is a generally useful technique since it is often easier to examine corrections at the canonical level. We have begun to perform some related benchmark calculations based on a novel implementation of a path integral based random sampling approach.[126] This approach, which effectively considers all aspects of the multidimensional fluxional mode

couplings, including for the inversions, has already been incorporated and tested in the AutoMech software. One important feature of this approach is that it does not involve expansions about each of the minima and so does not require the determination of all minima on the potential energy surface. Indeed, demonstration calculations for n-dodecane have already proven to be feasible with direct ab initio sampling of the torsional potential. One drawback of this approach is that the results converge more slowly at lower temperatures, but for combustion temperatures (e.g., 700 K and higher) convergence appears to be efficient enough. Such benchmark calculations should find utility in developing and test simpler approaches.

2.2 Criegee Intermediates

The Lester group has also used their novel jet cooled IR action spectroscopy approach to observe the dissociation rates for a large set of Criegee intermediates (CIs).[56,115,127-129] These species, which are formed in the atmosphere through the ozonolysis of alkenes, are of considerable importance as a source of OH radicals. The key first step in this process generally involves an intramolecular H transfer to form a vinyl hydroperoxide species, with a low barrier that is commonly in the 15 to 20 kcal mol^{-1} range.[130] The OO bond in the incipient vinylhydroperoxide (VHP) is readily split to yield OH and an alkoxy radical at an energy that is below that of the H transfer barrier. Lester's experiments use LIF to observe the time dependent appearance of the OH after IR induced excitation to specific vibrational states of the CI.

A priori tunneling corrected RRKM predictions for the rates have been compared with the energy resolved rate constants for the whole series of CIs [CH_3CHOO, CD_3CHOO, $(CH_3)_2COO$, CH_3CH_2CHOO, $CH_3CH_2C(CH_3)OO$, $CH_2CHC(CH_3)OO$, and $CH_3CHCHCHOO$] studied by Lester and coworkers. The rate predictions were found to be in excellent agreement with the experimental observations, with the differences rarely being outside the estimated experimental error bars. The agreement across the series validates both the statistical RRKM model for this class of reactions, as well as our specific ab initio implementation of it. Clearly, the ANL0 predictions for the barrier heights are highly accurate.

2.2.1 Tunneling

For the CH_3CHOO and $(CH_3)_2COO$ dissociations the observations spanned a broad range of energies from the deep tunneling regime (~ 5 kcal mol^{-1} below the barrier) to energies in the neighborhood of the barrier. Notably, even near the barrier, the tunneling corrections were predicted to be significant, with good agreement between SC-TST and Eckart estimates extending down into the deep tunneling regime. The accurate prediction of the rate for both CH_3CHOO and CD_3CHOO, where there is a kinetic isotopic effect of ~50, provides a clear indication of the importance and accuracy of the tunneling correction.[57]

2.2.2 Resonance Stabilization

The ozonolysis of isoprene, which is the second most abundant volatile organic compound in the Earth's troposphere (after methane), yields a mixture of three CIs: CH_2OO, methacrolein oxide [MACR-OO; $CH_2=C(CH_3)CHOO$] and methyl vinyl ketone oxide [MVK-OO; $CH_2CHC(CH_3)OO$].[131] MACR-OO and MVK-OO exhibit resonance stabilization of their CC and

CO π-bonds, which modifies their chemistry. Lester and coworkers observed the *E*-resolved decomposition kinetics for the MVK-OO case, as well as for 2-butenal oxide ($CH_3CHCHCHOO$), which is also resonantly stabilized. The latter CI is of interest because it is predicted to isomerize by a 1,6-H-transfer instead of the usual 1,4-H-transfer mechanism of smaller CIs.[132]

For the *syn*-MVK-OO case, the resonance stabilization of the reactant results in a H-transfer barrier of 18 kcal mol^{-1}, which is ~2 kcal mol^{-1} higher than in the non-resonantly stabilized cases we have studied.[128] Meanwhile, the 2-butenal oxide case occurs in two steps, with the first stage involving a low barrier (8 kcal mol^{-1}) conformational isomerization, and the second stage involving an even lower barrier (5 kcal mol^{-1}) H-transfer. The remarkably small barrier for this 1,6-H-transfer,[129] yields a much faster CI decomposition rate in agreement with earlier predictions of Vereecken for the thermal rates.[132]

2.2.3 Stereochemistry

One aspect of unimolecular reactions that is highlighted by the Criegee intermediate observations is that the kinetics is strongly dependent on the stereochemistry of the reactants.[128,130] For example, the syn and anti isomers of many CIs have vastly different dissociation rates, and products. In MVK-OO the *syn* form reacts via H transfer from the CH_3 group to the terminal O atom. In contrast, the *anti* form reacts via 5 membered ring formation and is predicted to have a thermal rate that is two orders of magnitude faster than that for the *syn* form.[128]

The importance of incorporating different rates for different stereoisomers has been recognized in recent theoretical calculations for both atmospheric[133-135] and combustion processes.[136,137] However, at least in combustion modeling, such effects have largely been ignored in the formulation of global chemical models. The large number of species and reactions present in a combustion model makes it challenging to convert a non stereospecific mechanism to one that properly includes the stereochemical nature of the conversions. We have recently developed scripts for automatically implementing such stereochemical expansions.[138] They are available as part of our AutoMech code.[107] One interesting challenge that was encountered in this work was a shortcoming in the InChI formalism for identifying the stereochemistry in resonantly stabilized radicals. We have developed a supplement to InChI, which we label AMChI, that properly handles such species. Notably, a paper by Rotavera and coworkers in this discussion meeting explores the stereochemical dependence of the reaction kinetics for the peroxy radicals derived from 2,4 dimethyloxetane.[139]

2.2.4 Multiple Transition States and Roaming in "Simple" Bond Fissions

Bond fission to produce two radicals was long thought to be a simple process that occurs over a monotonically rising minimum energy path potential, i.e., without a reverse barrier. However, in reality, this is rarely the case. Instead, most pairs of radicals have some form of weak hydrogen-bonded or van der Waals long-range complex that exists as a minimum on the potential energy surface at large separations (typically about 3 Å separation). The optimal orientation of the two radicals in that long-range complex generally differs quite significantly from that in the chemically bound molecule. Correspondingly, there is a transition state (typically at about 2-3 Å bond separation) that correlates with the required reorientation of the radicals for the transition

between the two complexes. From the long-range complex, gradually increasing the separation between the incipient fragments yields a monotonically increasing potential energy. Nevertheless, there is also a transition state for this final separation of the two fragments. It correlates with an entropic minimum for the relative bending motions, arising in part from the effect of centrifugal barriers. We label these two transition states as the "inner" and "outer" transition states for the bond fission process.

The quantitative description of the radical-radical interaction energies in this long-range region of configuration space, is challenging. Single reference-based methods are not applicable. We generally find that the CASPT2 (second order perturbation theory applied to a complete active space reference wavefunction) and MRCI+Q (singles and doubles multi-reference configuration interaction with Davidson corrections for higher order excitations) methods provide effective means for exploring the interactions in this long-range "roaming" regime. We also find that a "trick" involving the use of multireference methods to evaluate the difference in energy between high and low-spin energies, and coupled cluster methods to evaluate the high-spin energies often provides the highest quality energies.[140]

In Fig. 6, we illustrate the calculated interaction energies for constrained optimizations in this long-range roaming region with fixed OO separation in the OO bond fission of CH_2CHOOH, which is the VHP that is produced by 1,4 H-transfer in CH_3CHOO. The 4-electron, 4-orbital active space employed in these CASPT2 calculations correlates with the two radical orbitals and the π,π^* orbitals of the CC bond. All the calculations employ the cc-pVTZ basis set of Dunning. The CASPT2 results show a saddle point at 2.4 Å separation with an energy that is 4 kcal mol^{-1} below separated radicals. A corresponding H-bonded minima occurs at an OO separation of 2.9 Å, with an energy of -9 kcal mol^{-1}.

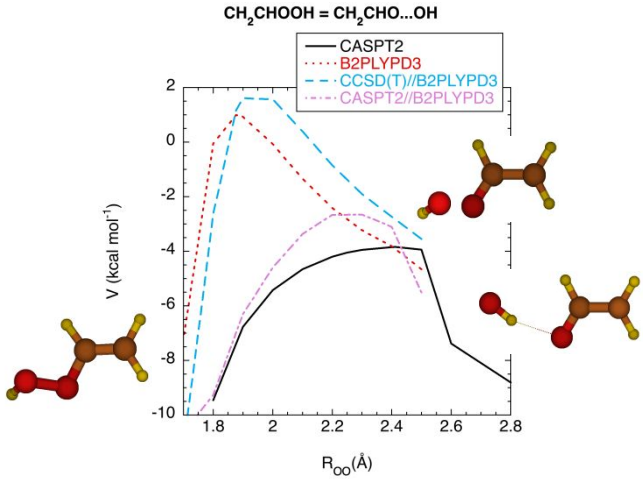

Fig. 6: Interaction energies along the distinguished coordinate minimum energy path for OO fission of CH_2CHOOH. The molecular structures depict reactants, transition state, and hydrogen-bonded complex.

The B2PLYPD3 and CCSD(T) results (which are calculated for the B2PLYPD3 geometries) in Fig. 6 demonstrate the limitations in standard single-reference methods (essentially equivalent results are obtained with other common functionals such as B3LYP and M062X). These calculations employ symmetry-broken unrestricted spin reference wavefunctions, which generally yields solutions that appear to show the qualitatively correct behavior (i.e., with a saddle point near zero-energy), but are from far quantitatively accurate. Unfortunately, such inaccurate approaches are still commonly employed in kinetic analyses of radical-radical reactions.

The CASPT2//B2PLYPD3 curve presented in Fig. 6 demonstrates that the primary problem is not in the geometries that are obtained with the symmetry-broken B2PLYPD3 method, but rather in the ability of single reference methods to quantitatively treat radical-radical

Fig. 5: Interaction energies along the OO bond fission distinguished coordinate minimum energy path for CH2CHOOH. The molecular structure depict the reactant, transition state, and long-range hydrogen bonded complex.

interactions at large separations. Nevertheless, the shift in the location of the saddle point from 2.4 to 1.9 Å from the CASPT2 to the B2PLYPD3 analysis implies errors of about -3 kcal mol^{-1} if the saddle point energy were to be obtained from a multireference analysis at the B2PLYPD3 saddle point, as is occasionally done. Meanwhile, a variational CASPT2//B2PLYPD3 analysis of the saddle point (i.e., with single point CASPT2 evaluations at each of the B2PLYPD3 optimized geometries) would only be in error by about 1.2 kcal mol^{-1}.

For many bond fissions, alternative paths from the long-range minimum are also accessible. In particular, an alternative reorientational or "roaming" motion of the radicals with respect to each other often connects two separate long-range minima. These new long-range minima are then often connected to an abstraction saddle point.[141] Alternatively, they may be connected to a separate molecular complex if one of the radicals is resonantly stabilized. The set of multiple transition states for partial fission, roaming, abstractions, and long-range separation adds considerable complexity to the classic picture of simple bond fission. Such roaming induced complexities are ubiquitous in the "simple" bond fission of neutral closed shell molecules. They occur essentially every time one of the incipient radicals is either resonantly stabilized or has an H atom that is easily abstracted. We have developed a simple statistical theory for treating the kinetics of such multiple transition state processes.[142] It involves the use of steady state approximations for each of the weakly bound intermediates.

In some dissociations, both ordinary tight transition states and roaming radical saddle points can exist for the same products. For those cases, second order saddle points generally exist and provide a connection between the two first-order saddle points.[143] In a paper presented at this meeting, Lourderaj and coworkers, use ab initio classical trajectory simulations to examine the influence of second-order saddle points on some sample reaction mechanisms.[144] A joint experiment-theory paper from Suits and coworkers provides an interesting exploration of the role of resonances in the roaming branching and of the dependence on the angular momentum state in the photodissociation of formaldehyde.[145]

The initial 1,4 H-transfer that occurs in the decomposition of many CIs is generally followed by OO bond fission of the VHP. The incipient alkoxy radicals are resonantly stabilized, and roaming isomerization then yields the possibility for hydroxycarbonyl formation. Notably,

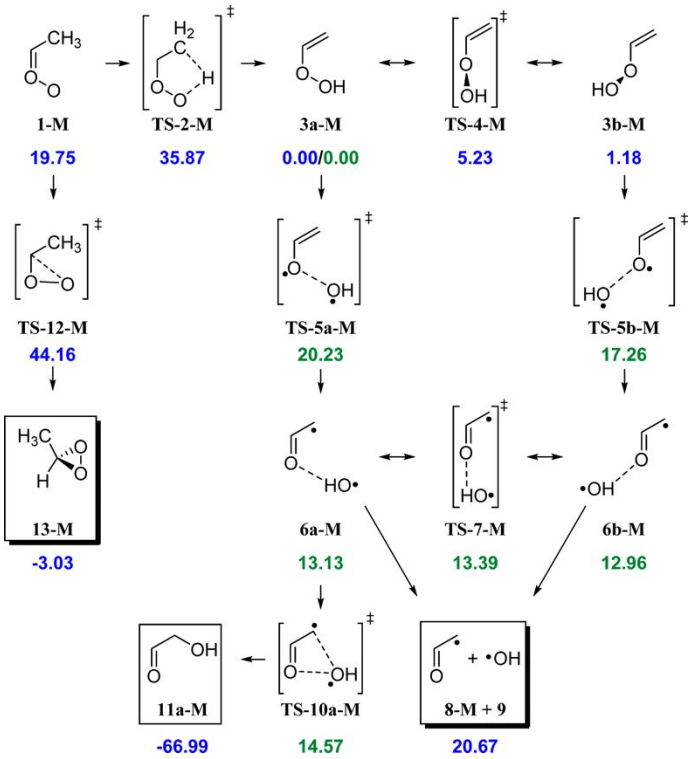

Fig. 7: Schematic reaction mechanism for the dissociation and roaming induced isomerization of CH_2CHOOH. Energies are in kcal mol^{-1} as described in Ref. *147*. Reprinted with permission from Ref. *147*. Copyright 2018 American Chemical Society.

an experimental study of the dissociation of $(CH_3)_2COO$ observed the formation of the hydroxyacetone product.[146] Subsequent theoretical work from Kuwata and coworkers provided an explanation for these observations in terms of the roaming induced mechanism as outlined above (cf. Fig. 7),[147] and provided estimated branching ratios for the formation of the hydroxyacetone at a range of temperatures and pressures of relevance to the troposphere. Notably, their analysis suggests that hydroxyacetone will account for 70% of the CI decomposition products at 200 K and 100 Torr.

We have reanalyzed the energetics in the roaming region for the smaller CH_3CHOO case (which Kuwata et al. also explored[147]) with a CASPT2 approach. We find good agreement with their results, with the primary distinction being the absence of the TS-5a saddle point in the CASPT2 analysis. Interestingly, this absence implies that the 6a hydrogen bonded complex, which is a key precursor to hydroxyaldehyde, is formed by roaming from 6b. Although not yet explored, one might also expect a roaming induced abstraction (to produce ketene + water) to be accessible from the vinoxy…OH long-range complexes.

In our collaborative study of the dissociation of syn-MVKOO with the Lester group we provided a similar exploration of the roaming path for this process.[128] Again in collaboration with Lester, Caravan, and others, we are now exploring this process in even greater detail for methylethyl CI, as described in a poster for this meeting.[148] Notably, in this case, the experimental effort was able to identify stable hydroxybutanone products, just as predicted by our mapping of the roaming induced isomerization pathways. Interestingly, in these VHP dissociations a multi-step sequence of two different roaming reactions may occur. In particular, simple CC fission may provide the lowest energy path for dissociation of the hydroxycarbonyl arising from roaming in the original VHP. For such CC fissions, a variety of roaming induced reactions are feasible. The net result is that the dissociation of a single CI may occur through first an H-transfer reaction followed by a two stage sequence of roaming reactions.

A key remaining experimental challenge for roaming radical reactions involves the detailed observation of the branching to the various product channels over a wide range of *E* and/or *T*. Our statistical kinetic roaming model should provide a qualitatively correct description of the branching, but there are indications that the dynamics of the intermediate weakly bonded complexes is not fully ergodic.[149] Experimental observations of the product branching from just below the threshold to formation of separated fragments to well above it would provide valuable benchmark data for testing of theoretical models. This product branching is expected to show dramatic dependence on *E* and *T*. Furthermore, for a dissociation with multiple possible roaming abstraction channels (e.g., CC fission in $OHCH_2CHO$), the observations over a range of sub-threshold energies would provide an interesting description of the competition between distinct roaming processes.

2.2.5 Prompt Dissociation

The kinetics of CIs also highlights another important aspect of unimolecular dissociations that has come to the forefront in recent years. In particular, there are many instances where one cannot consider the dissociation of a species in isolation. Instead, the species decomposition rate as well as the distribution of its product species can be strongly dependent on how that species is

first formed. For example, if the formation process is highly exothermic, the subsequent dissociation may occur more rapidly than the collisions that are required to form a thermal distribution. In such "prompt" dissociations, the dissociation rate and product branching will not be well modelled by the standard solution of the master equation for a thermal distribution.

The ozonolysis that leads to the formation of CIs is highly exothermic. For example, for ethylene the ozonolysis to yield CH_2OO + H_2CO is 48 kcal mol^{-1} exothermic.[150] There is also a small branching to a ketohydroperoxide (KHP; $OCHCH_2OOH$) product (12%), which is 101 kcal mol^{-1} exothermic.[150] With this high an exothermicity for the KHP forming channel, and no companion product to take away the excess energy, it will all promptly dissociate to $OCHCH_2O$ + OH. Meanwhile, the lowest dissociation barrier for the CI is at 19.1 kcal mol^{-1},[151] and the probability for prompt dissociation then depends strongly on the fraction of the reaction exothermicity that is deposited into the CI. This prompt dissociation of CIs is well known, and considerable effort has been invested in the development of schemes for predicting the fraction that thermalizes prior to stabilization [known as the stabilized CI (sCI) yield].[152]

One of the challenges in predicting the sCI yield theoretically is that one cannot simply use statistical theories to predict the partitioning of energy into the separate fragments. The validity of RRKM theory for rates says nothing about the extent of energy flow from the saddle point out to products. Furthermore, the decomposition of the primary ozonide that acts as a precursor to the CI formation is a highly multireference problem with a diradical pathway accessible in the same energy range as the CI forming channel. In a recent study,[150] we used direct trajectory simulations of the primary ozonide decomposition to explore the energy partitioning into the CI (cf. Fig. 8). We then combined these partitioning estimates with master equation simulations of the prompt dissociation probabilities to yield predicted sCI yields and also quantitated the uncertainties in our approach. There are essentially two ranges of experimental values for this quantity, with our prediction of 48% sCI yield, falling well within the higher set of experimental values.

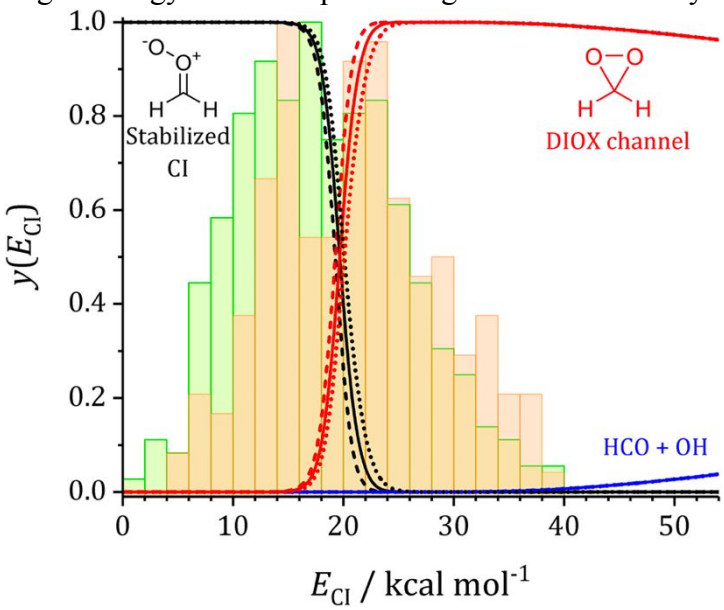

Fig. 8. Energy dependent yields of sCI (black), dioxirane (red), and HCO + OH (blue) from master equation modeling. The dashed, solid, and dotted curves denote results for energy transfer parameters of 110, 170, and 260 cm^{-1}, respectively. The green and orange histograms denote the CI rovibrational distributions predicted for concerted and stepwise pathways, respectively. Reprinted from Ref. 150 with the permission of

A recent study of α-pinene oxidation provides a spectacular example of how complex the process of prompt reactions can be.[153] In particular, the ozonolysis of α-pinene leads to a CI that promptly isomerizes to a VHP. The VHP then promptly dissociates to OH plus a vinoxy radical,

which in turn promptly performs a ring-opening isomerization. This sequence of 3 prompt processes was necessary to rationalize the observed production of ring opened products. Interestingly, although not examined in that work, the VHP decomposition might also involve a roaming radical induced isomerization since the vinoxy radical is resonantly stabilized. Similarly, there is also a readily abstracted H atom in the vinoxy, so there might also be a roaming induced abstraction from it. Furthermore, the hydroxyketone would also be subject to further prompt and roaming reactions. It is truly remarkable how complex the sequence of conversions can become.

Such prompt dissociations are also ubiquitous in combustion chemistry. For example, many radicals are formed via exothermic abstractions of an H atom from a fuel molecule. The combination of the low binding energies for radicals, the high temperatures of combustion, and the excitation of the radicals via the exothermicity of their formation reactions results in a significant probability for prompt dissociation of the radicals. Indeed, for high temperatures combustion modellers have found it useful to simply replace the radicals with the products of their breakdown reactions.[154]

Sivaramakrishnan and coworkers performed a detailed study of the probability and importance of such prompt dissociations for the HCO radical.[155] This radical plays a key role in combustion, with the branching between its dissociation and further reaction with O_2 playing an important role in determining the flame speed. The coupling of direct trajectory simulations of the abstraction induced energy distribution with master equation simulations of the HCO decomposition process indicates that the prompt dissociation gradually rises in significance starting at about 800 K and reaching 50% probability by about 2000 K. The inclusion of these prompt dissociation probabilities in global combustion models indicated up to a 15% increase in the flame speed (cf. Fig. 9), which has important ramifications for practical modeling purposes.

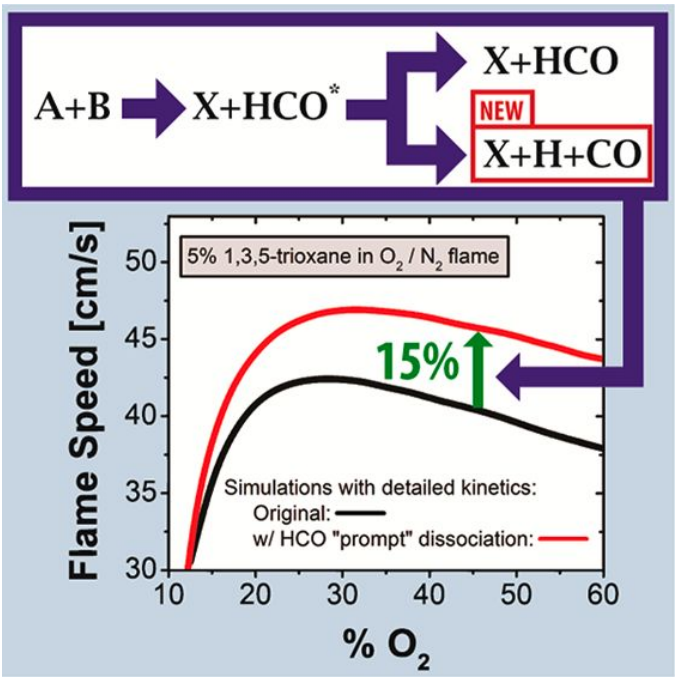

Fig. 9. Plot of the effect of prompt dissociation of HCO on modeling of 1,3,5-trioxane flame speeds. Reprinted with permission from Ref. *155*. Copyright 2016 American Chemical Society.

Prompt dissociations also play a key role in the sequence of radical oxidation reactions that lead to chain branching in low temperature oxidation.[156] For example, in a collaborative study of diethyl ether oxidation with Goldsmith we explored the coupled sequence of prompt dissociations of first the O_2QOOH, then the KHP, and finally the ketoalkoxy radicals.[157] This sequence had a strong effect on the chain branching through an effective increase in the KHP dissociation rate, as well as in the final product branching from the ketoalkoxy decomposition. Notably, the importance of the prompt processes increased significantly as more reactions were included in the prompt analysis sequence. The predicted broadening and shift in the production of

acetic acid to lower temperature improved the agreement with the observations from jet stirred reactor experiments.

It is time consuming to estimate the energy distributions with trajectory simulations. In general, one expects that a radical will be formed with at least a thermal distribution of energy states. Notably, even such thermal distributions contain some probability for prompt dissociation because the steady state distribution of dissociating molecules is depleted in states near the dissociation threshold, whereas an incipient thermal distribution is not. The prompt dissociation probability for a thermal distribution turns out to be identical to what has come be known as the nonequilibrium factor, f_{ne}.[158]

Statistical approaches provide an alternative means for predicting the energy distribution of the nascent radicals. Various statistical limits were considered in our study of the alkene ozonolysis process.[150] Goldsmith and coworkers also considered a number of possible statistical distributions.[159] The sudden vector projection model of Guo and coworkers provides an alternative estimate that is based on mode projections at the saddlepoint.[160] We have now implemented a number of these approaches into our AutoMech software suite.[107] It will be interesting to explore the suitability of these models for various reactions. One expectation we have is that the fully statistical model will prove more effective for larger more complex molecules, particularly for ones with stronger hydrogen-bonding interactions in the long-range region. One interesting preliminary finding is that the fully statistical models lead to greatly enhanced prompt dissociation effects over f_{ne} based estimates.[161]

Currently, the coupling of an arbitrary sequence of dissociations initiated by a single bimolecular reaction has been implemented and is being tested within AutoMech.[161] The inclusion of a sequence of bimolecular reactions is a bit more complicated due to the need to couple multiple PESs in order to properly treat the dissociations back to reactants. Lei and Burke recently presented an approximate methodology for handling that process together with a set of scripts for doing so.[162] Earlier work by Roberston and coworkers presented a fully reversible method for doing so.[163,164]

2.2.6 Hot reactions

The preparation of molecules with an excess of energy in their internal states can also lead to an enhancement of their bimolecular reaction rates. For example, the abstraction of an H atom from CH_4 by standard abstractors (e.g., OH, H, or O_2) is greatly increased when the CH_4 itself is highly excited in energy. Thus, any consideration of the effect of prompt dissociation should also consider the increase in the species bimolecular reaction rates. Of course, for such effects to be important, the bimolecular reactions need to be competitive with the collisional cooling process.

For the recombination of CH_3 with H to form chemically activated CH_4, Jasper et al. demonstrated with trajectory calculations that the rates of such hot bimolecular abstractions are indeed enhanced by orders of magnitude and do compete with the collisional cooling process.[165] A follow on study led by Sivaramakrishnan explored related effects for chemically activated H_2O reactions and showed that the inclusion of such hot bimolecular reactions can significantly effect global combustion properties such as the flame speed.[166] A separate study with Burke indicated that the chemically activated complex does not even need to be long lived for its reactions to have

a significant impact on the global kinetics.[167] In particular, chemically termolecular H + O_2 + X reactions (X = H, O, and OH) significantly enhance the net rate of H loss in H_2/O_2 flames. As a result, the flame speeds were predicted to significantly decrease.

As discussed by Plane and Robertson, optical transitions can also lead to vibrational disequilibrium. For this meeting, they use master equation simulations to demonstrate that such vibrational nonequilibrium can increase the predicted concentration of metal silicates in oxygen-rich AGB stars by 6 orders of magnitude.[168]

In a paper at this meeting, Burke et al. describe yet another unexpected affect that arises for hot reactants.[169] In particular, the steady state distribution of dissociating molecules is depleted in energy states near and above the dissociation threshold. This depletion, which is increasingly significant at lower pressures, implies that the presumed "thermal" distribution of states for the molecules bimolecular dissociation is inaccurate. Correspondingly, one expects a decrease in the bimolecular rate constant from that predicted by standard transition state theory, with this decrease becoming increasingly significant with decreasing pressure.

Meanwhile, the paper of Xu and coworkers, provides another example of a situation where a bimolecular abstraction reaction is pressure dependent.[170] In this case, the pressure dependence arises from partial stabilization of a van der Waals complex between the two reactants. Related descriptions of pressure dependent bimolecular reaction rates arising from partial stabilization of a weak precursor complex have been presented by Canosa and coworkers[171] and by Nguyen and Stanton.[172]

2.3 RO_XR'

The decomposition of oxide molecules, RO_XR' with x=2, 3, or 4, provide an excellent example of the full complexity of dissociation dynamics for a reaction with just a single well. These species arise in the self and cross reactions of RO, RO_2, and R, and are important in both atmospheric and combustion environments. Their unimolecular decomposition generally begins with a partial fission of one of the OO bonds to produce some form of hydrogen bonded intermediate. A wide assortment of reaction channels are then accessible from these hydrogen bonded complexes. However, access to many of these channels requires various combinations of roaming and intersystem crossing processes. Furthermore, quantitative treatments of their energetics require multi-reference wavefunction based methods, and the treatment of the channel specific kinetics is similarly challenging due to the strong anharmonic couplings of the interfragment modes.

For a peroxide complex (RO_2R'; formed from the reaction of RO_2 with R' for example), the initial partial OO fission yields a singlet RO…OR' complex, and the possible products are relatively simple. In particular, roaming induced abstractions from this hydrogen bonded complex can yield $R_{-H}O$ + R'OH or ROH + $R'_{-H}O$. Meanwhile, complete fission simply yields RO + R'O. In this case, there may also be some intersystem crossing to a triplet RO…OR', but the dissociation of this triplet intermediate simply contributes to the RO + R'O flux.

Meanwhile, for a trioxide complex, RO_3R', initial OO fission can yield singlet and triplet $RO_2…OR'$ as well as singlet and triplet $RO…O_2R'$ complexes. Notably, intersystem crossing should yield rapid equilibration of the singlet and triplet states due to the near degeneracy of the singlet and triplet hydrogen bonded complexes. Roaming induced abstractions from the singlet $RO_2…OR'$ complex may yield $RO_2H + R_{-H}O$, or $R_{-H}O_2 + R'OH$, while continued separation of the fragments will simply yield $RO_2 + R'O$. Interestingly, the $R_{-H}O_2$ complex is typically a Criegee intermediate, or if R is an H atom, then it is $^1O_2$. In the H atom case, the dissociation of the triplet $RO_2…OR'$ complex may yield $R'OH + {}^3O_2$. Following the analogous paths from the $RO…O_2R'$ hydrogen bond complexes, suggests that $R_{-H}O + R'O_2H$, $ROH + R_{-H}'O_2$, $RO + R'O_2$ and $ROH + {}^3O_2$ may also be formed.

The set of feasible channels is even larger for tetraoxides, RO_4R'. In this case, initial OO partial fissions can yield singlet and triplet $RO_3…OR'$, $RO…R'O_3$, and $RO_2…R'O_2$ complexes. Again, one can have roaming induced abstractions and complete fission channels from each of these complexes. However, in this case the RO_3 fragments are generally metastable and may partially dissociate within the $RO_3…OR'$ complex (or from within the $RO…R'O_3$ complex) to yield $RO…O_2…OR'$. This complex may exist in singlet, triplet, or quintet states, with rapid intersystem crossing expected between them all. From this complex, roaming induced H abstractions are again accessible (cf. the channels discussed for the RO_2R' case), with these channels perhaps occurring before or after departure of $^1O_2$ or $^3O_2$. Notably, the $^3O_2$ production does not even require intersystem crossing since the triplet spin of the O_2 could be balanced by formation of a $^3RO…OR'$ complex.

A number of recent experimental and theoretical studies have examined the kinetics of formation and decomposition of the RO_XR' molecules. For the $RO_2 + OR'$ reactions, there has been considerable recent interest in the branching between stabilization of the RO_3R' and the various bimolecular products.[173-178] For the $HO_2 + HO_2$ reaction, we demonstrated the importance of the previously neglected formation of $OH + OH + O_2$ to combustion kinetics.[179] For this meeting, Kuwata et al. discuss new calculations for the reaction of acetylperoxy with HO_2.[180] Recent theoretical studies of $RO_2 + R'O_2$ are beginning to explore the full complexity of the kinetics, although there is still progress to be made.[181-185] There was also a recent attempt to develop a structure activity relation for the related reactions.[186] The development and validation of quantitative models for those complex unimolecular dissociations would be a major accomplishment for the modeling of unimolecular dissociation kinetics.

The singlet triplet nonadiabatic crossings are important features of the RO_XR' dissociations. For this meeting, Guo and coworkers considered the nonadiabatic dissociation dynamics of electronically excited HCO. Their study finds an interesting modulation of the nonadiabatic decay rate through a combined experimental-theoretical study.[187] Meanwhile, a combined experiment and theory study of Cavallotti et al. explores the effect of nonadiabatic crossings on the reaction of $O(^3P)$ with 1,3-butadiene. The good agreement between theory and experiment for this study provides a nice illustration of the complexity of system that can now be quantitatively treated with AI-TST-ME models that include the effects of nonadiabatic transitions. It is perhaps worth noting that while an effective treatment of intersystem crossing within nonadiabatic statistical theory, even including multidimensional corrections,[188] is reasonably straightforward, the treatment of

internal conversion is much more challenging. In particular, the latter case commonly involves delocalized, history-dependent transitions that demand a dynamical treatment.[189]

3. Pressure Dependence

A neglect of the pressure dependence for unimolecular reactions is a common shortcoming in large scale chemical modeling. Notably, our ability to provide accurate a priori treatments of this pressure dependence has improved dramatically in recent years. A paper presented by Van Geem and coworkers at this meeting provides a nice illustration of the importance of replacing high pressure limit rate constants with proper pressure dependent expression in the modelling of steam cracking.[190] In this section we briefly overview some of the recent progress in the methodologies for predicting this pressure dependence.

3.1 Collisional Energy Transfer

The treatment of the pressure dependence via the master equation requires some prescription for the rate of collision induced transitions in the state of the molecule. Within a statistical framework the state of the molecule is defined by its total energy E and total angular momentum J, since those are the only two quantities that are conserved between collisions. Thus, within that framework, the requisite collision kernel should describe the rate of transitions in E and J. However, to simplify the calculations, one commonly presumes that the effect of the transitions in J can be averaged over, and the collisional analysis focuses solely on the transitions in E.

Over time, a practical approach to one dimensional (in E only) master equation modeling developed around the combination of Lennard-Jones collision rates, k_c^{LJ}, coupled with an "exponential down" model for the probability of a given energy transfer in each collision. For a transition from state E to state E' the collision kernel is written as

$$k_c(E,E') = k_c^{LJ} \exp[-(E-E')/\alpha] \qquad \text{for } E > E'$$

The expression for upwards transitions is obtained from that for downwards transitions via microscopic reversibility.

With this expression, the parameter α correlates with $\langle \Delta E_{down} \rangle$, the average energy transferred in all collisions that transfer energy from the molecule to the bath gas. This quantity depends on both E and T. The dependence on T is commonly represented as a power law:

$$\alpha = \alpha_{298} \, (T/298)^n$$

Incorporating this T dependence is important when modeling dissociation rates from room temperature all the way up to combustion temperatures. In contrast, the E dependence of α is usually of little significance and is often ignored. In effect, the collision kernel plays a significant role in determining the dissociation rate only for E near the dissociation threshold. Over this range of energies, the variation in $\langle \Delta E_{down} \rangle$ is typically quite mild.

Nevertheless, as the precision of theoretical predictions improves, it may become important to consider this variation. This concern will be particularly important for reactions with energetically distinct barriers. Notably, Barker has long argued for the use of energy dependent α parameters as a means to obtain more stable master equation solutions, especially at lower energy.[191] Perhaps more importantly, he has also noted that some variation is in better accord with experiment. Truhlar and coworkers have recently discussed the significance of such energy dependent α parameters.[192]

The parameters α_{298} and n depend on the specific molecule and collider. Historically, these values have been determined from fits to experimental data, with α_{298} generally larger for larger molecules, and for colliders that interact more strongly with the dissociating molecule. Typical values for α_{298} range from about 50 to 500 cm^{-1}. With the current substantive body of fitted and calculated α_{298} values one could make empirical estimates with uncertainties of about a factor of 1.5 to 2. Meanwhile, the parameter n commonly takes values between 0.5 and 1, but its variation with molecule is much less well understood.

It is important to recognize that the primary utility of the Lennard-Jones plus exponential down procedure for predicting dissociation rates is as a model for fitting and extrapolating data. The presence of dipolar and other strong interactions suggests that one should really employ collision rates that are larger than the LJ collision rate. The use of k_c^{LJ} can lead to challenges in fitting data for strong colliders with large average energy transfers. Meanwhile, the assumption of an exponential form may not be flexible enough to fit the energy transfer probability over a broad range of energy. This limitation can lead to challenges in fitting/predicting data for multiple channel reactions. Lastly, it is not clear how the neglect of J conservation, and anharmonicities in state densities affects the fitted values. Nevertheless, the approach has proven remarkably effective for "predicting" (more precisely extrapolating and interpolating) the T and P dependence of simple one channel dissociations. To some extent, this success has hindered the use of more accurate representations, since that would negate some of the utility of the empiricism developed over time. But, for more complex MWMC reactions, there is a considerable cause for caution in interpreting the results of such calculations.

Jasper made a bold step beyond the historic empiricism of this Lennard-Jones plus exponential down procedure when he began directly calculating $\langle\Delta E_{down}\rangle$ with trajectory simulations.[193] He has now mapped out $\langle\Delta E_{down}\rangle$ as a function of temperature for a wide range of molecule types and sets of bath gases.[194,195] A new set of data for water as a collider is included in his paper for this meeting.[196] This latest analysis focusses on the low-pressure limit, which Jasper argues provides an effective regime for considering collider effects.[196,197] Matsugi has presented examinations for the bath gas dependence of unimolecular decomposition reactions for a few different reactions.[198,199] You and coworkers recently presented related calculations for PAH molecules.[200] It also worth noting that Jasper's analysis employs some of his recent strategies for efficiently generating high quality intermolecular potentials, which are key to obtaining quantitative predictions.[201,202]

Jasper's trajectory calculations for CH_4 yielded α parameters that were about two times larger than those obtained empirically, once anharmonicity was accounted for. This discrepancy highlights the empirical nature of prior master equation modeling efforts, although there was also

some possible concern about a role for quantum effects in energy transfer. However, this seemed unlikely given the high energy states of the molecules and a more likely explanation lay in the neglect of angular momentum within the 1DME.

3.2 Angular Momentum and the 2DME

Within the 1DME there is considerable ambiguity regarding how best to average over the total angular momentum. Naively, one might simply replace the *E,J*-resolved numbers and densities of states with their *J*-integrated analogues. This standard 1DME approach corresponds at least qualitatively to presuming *J* is thermally randomized after each collision. Presuming instead that the product *J* value after a collision is statistically distributed for a microcanonical distribution yields a different result that is slightly more justified physically.[203,204] Notably, with that presumption the *J* part of the 2DME can be integrated over analytically. This approach came to be called the 2D/φ model, although I prefer 1D/microcanonical-*J* model. More recently, an opposite limit for the *J*-averaging has been pursued by Stanton and coworkers.[205] In particular, they presume that collisions have no effect on the *J*-distribution. They then perform 1DME simulations for the full range of *J*-values and average over the results from each of those *J*-dependent simulations. Stanton and coworkers also like to call this approach a 2DME approach, but I think a better label would be 1D/fixed-*J* to better emphasize the nature of the assumption about the *J* part of the collision kernel. Similarly, their recent "3DME" approach, which includes *K* conservation (where *K* is the projection of *J* on the body-fixed axis), would be better labelled as 1D/fixed-*J*,fixed-*K*.[206] Clearly, neither the 1D/microcanonical-*J* or 1D/fixed-*J* models are physically correct and the proper solution should lie somewhere between these limits.

In collaboration with Jasper we explored the issue of the proper treatment of *J* through 2DME calculations employing collisional transfer kernels directly determined from trajectory simulations. Smith and coworkers had already demonstrated the feasibility of solving the 2DME numerically.[207,208] Meanwhile, Barker and Weston had nicely explored the 4-dimensional collisional transfer kernel $P(E,J;E',J')$ with trajectory simulations for some sample dissociative systems.[209] Building from these works, we developed a novel representation of the collisional kernel that was focused on accurately reproducing the trajectory determinations of the lowest few moments of the distributions in ΔE and ΔJ.[210] Implementing this form in the 2DME for the CH_4 and C_2H_3 reaction systems yielded remarkably good agreement with experimental data[211] obtained over a wide range of conditions

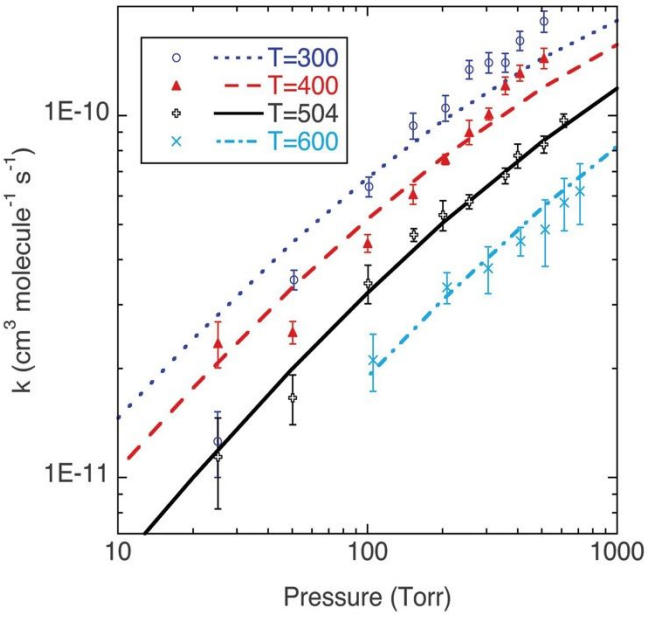

Fig. 10: Plot of the full 2DME a priori predictions (lines) for the pressure-dependent rate constant for $CH_3 + H \rightarrow CH_4$ for a variety of temperatures, all with He as a bath gas. Symbols denote experimental results from Brouard et al.[211] From Ref. 210. Reprinted with permission from AAAS.

(cf. Fig. 10). This good agreement demonstrated that the trajectory simulations were indeed providing accurate predictions of the collisional transfer kernels, and that the real problem lay in the assumption of microcanonical strong collisions in *J*. Experimental efforts to resolve the *J*-dependence of energy transfer probabilities, such as the one on CO energy transfer presented by Mullin and coworkers at this meeting,[212] are helpful in better understanding the full 2-dimensional transition kernels.

Matsugi has recently presented an alternative approach to implementing 2DME simulations in combination with a trajectory based analysis of the *E,J* collision induced transition kernel.[213] His most recent analysis includes a treatment of channel switching in three separate sample reactions.[214] Stanton and coworkers have also begun performing full 2DME simulations[215] including for the dissociation of C_2H_5 as part of this meeting.[71] Although, the *E,J* transition kernel is never specified, the discussion seems to suggest that the *E, J* components of the kernel are presumed to be separable. Furthermore, that is the presumption that was made in their earlier work. Exponential down representations of the individual *E* and *J* components of the kernel are obtained empirically.

Further work is needed to validate the forms for the *E,J* transition kernel of Matsugi and or Stanton and coworkers. Notably, our comparisons for CH_4, C_2H_3,[210] HO_2,[216] and QOOH[60] together with the new results presented by Jasper at this meeting,[196] demonstrate the success of our representation of the *E,J* transition kernel for single channel reactions. The limited attention paid to the high-energy tail in all of these representations suggests the need for careful testing and validation of *E,J* transition kernel forms for multichannel reactions with energetically separated reaction thresholds. The inclusion of a fit to the second order moments within our form may be enough to handle such effects, but that remains to be demonstrated.

The implementation of the 2DME approach can be somewhat time consuming. Thus, it is useful to have simple procedures to correct for the limitations in the existing 1DME models. Empirically, it seems that simply reducing the calculated $<\Delta E_{down}>$ value by a factor of 2 within a 1DME calculation often provides a reasonably effective approximate approach. Alternatively, a better approach is to properly evaluate the 2DME result in the low pressure limit, and then use that to renormalize the $<\Delta E_{down}>$ values employed in 1DME calculations of the full pressure dependence.

The latter approach was used in our AI-TST-ME calculations of the temperature and pressure dependence of the QOOH dissociation rates,[60] which were found to be in quantitative agreement with the available experimental data[217] (cf. Fig. 11). Interestingly, even in these thermal calculations, we see an important (factor of 2) contribution from heavy atom tunneling. Furthermore, when extrapolated to temperatures of relevance to combustion modeling, the predicted pressure dependence as well as the high pressure limit deviate quite significantly from those employing a 1DME based on fits to the same set of thermal experimental data.

3.3 Multiple Collider Effects

Typically, in a master equation calculation one considers the collisions with a single bath gas. However, in complex chemically reactive systems there are often a number of major species

present, and the composition of these species can evolve with the progress in reaction. For example, in a combustion environment, the reaction progress can lead to a significant fraction of H_2O and CO_2 being produced. Furthermore, the collider efficiencies for H_2O and CO_2 are often much larger than those of O_2 and N_2. Meanwhile, the fuel itself may initially be present at significant mole fraction, before it is gradually converted to products.

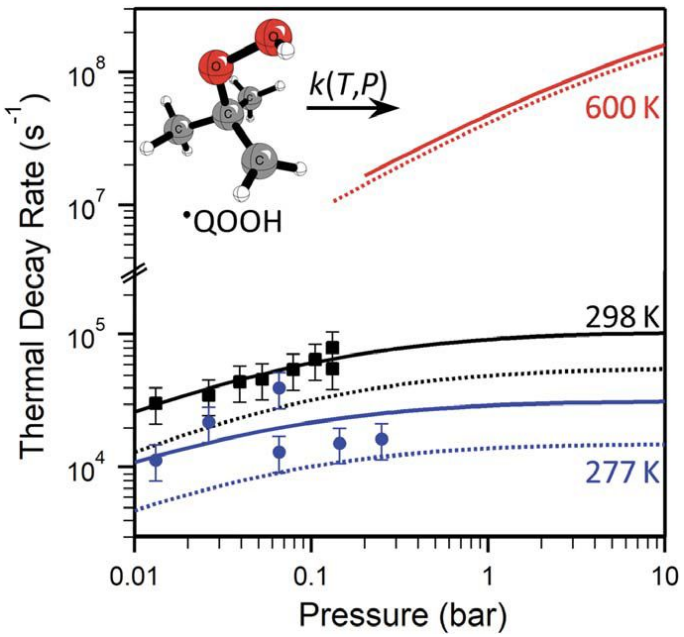

Fig. 11: Pressure-dependent thermal rates for unimolecular dissociation of hydroperoxyalkyl radical intermediates (•QOOH) with N_2 bath gas [at 277 K (blue), 298 K (black), and 600 K (red)]. The master equation predictions are with (solid) and without heavy-atom tunneling (dashed). The experimental data (symbols) are from Ref. 217. From Ref. 60. Reprinted with permission from AAAS.

In global kinetic models it is commonly presumed that the effect of a mixture of bath gases on the rate constant can be expressed as a linear sum of the effects of contributions from each of the bath gases considered in isolation. The MESS master equation code allows for the implementation of arbitrary combinations of colliders with separate collisional and energy transfer parameters. In a series of studies, Burke and coworkers have used this code (together with its predecessor VariFlex) to examine the appropriateness of the linear mixture rule for a variety of reactions and collider cases.[218-223] They find that the deviations from that assumption are often very large, and certainly need to be accounted for in realistic simulations. They also provide alternative representations that should provide a more accurate description of the multiple collider effects. It is perhaps worth mentioning that such multiple collider effects can have important ramifications for attempts to extract collider efficiencies from some kinetics experiments where mixtures of bath gases were used.

3.4 Lennard Jones Collision Rates

The uncertainty in the Lennard-Jones collision rates is generally much less than that of the energy transfer probabilities. Nevertheless, it is worth calculating those values with sufficient accuracy that their contribution to the overall uncertainty is negligible. Jasper and Miller have developed and implemented effective procedures for calculating these parameters and the related binary diffusion coefficients.[224,225] Global kinetics models general employ tables of Lennard-Jones parameters for the pure species and then obtain values for mixtures via simple combining rules. This situation is unfortunate, as such combining rules yield values that are significantly less accurate than could be calculated.[226]

A general code for automatically implementing Jasper's "OneDMin" spherically averaged procedure is available and is also directly integrated into our AutoMech software suite.[227] A large

number of values are now available with this approach. A paper at this meeting from You et al. explores an alternative "η-ξ" method for calculating the Lennard-Jones parameters.[228] This method aims to represent both the repulsive and attractive aspects of the potential and is also accurate and efficient.

3.5 The Low Pressure Limit

A recent paper from Truhlar and coworkers[229] highlighted the fact that in certain situations the low *P* limit behavior of the unimolecular decomposition rate is not actually linear in *P*. In particular, when there are two or more product channels the falloff in the rate constant for the slower channels is superlinear. This greater than linear decrease arises from the extra depletion by the faster dissociation channel of the excited energetic states of relevance to production of the slower channel. The study of Ref. 229 also discussed the interesting effects of competition between multiply connected species.

The inclusion of tunneling through the barrier also has important impacts on the low *P* behavior of the dissociation rate constant. In effect, with tunneling, the low *P* limit is not reached until the collision rate is less than the tunneling rate at the reaction exothermicity. This leads to a very slow approach to the low pressure limit when the reaction exothermicity is much less than the barrier height. In contrast, in the absence of tunneling, the linear in *P* behavior is reached as soon as the collision rate is lower than the dissociation rate at the barrier top. For formaldehyde dissociation (cf. Fig. 12) the effect is particularly dramatic. For a calculation with tunneling excluded, the rate constant approaches the linear in *P* low pressure limit by a pressure of about 0.01 bar. In contrast, with tunneling, there is no sign yet of linear in *P* behavior even at a pressure of 10^{-12} bar. The formaldehyde dissociation also clearly illustrates the superlinear falloff behavior for the dissociation to the higher energy/slower channel to produce H + HCO.

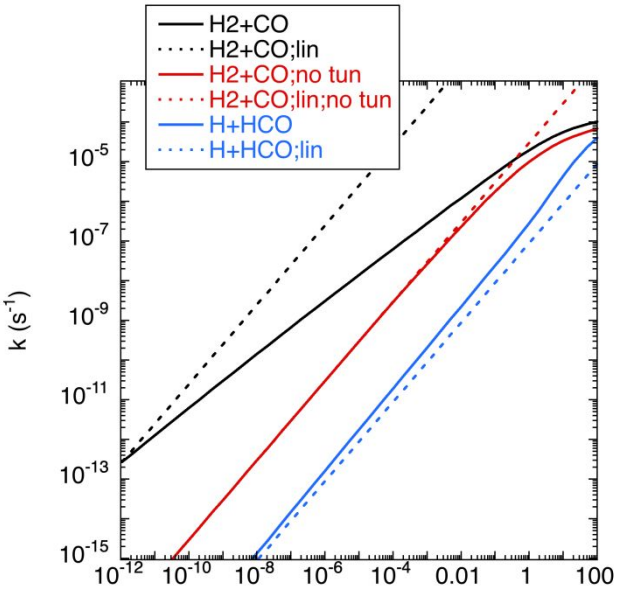

Fig. 12: Plots of the pressure dependence of the unimolecular dissociation rate constant for H_2CO at 1000 K. The dotted lines depict the expected linear in P limit starting from the rate at 10^{-12} bar. The black and red lines denote calculations with and without tunneling, while the blues lines denote the results for the higher energy H + HCO channel.

Radiative processes provide perhaps the strongest limit on the appearance of a linear *P* low pressure limit behavior. In particular, at low enough pressures radiative processes provide energy transition rates that exceed those of collisions. As a result, the true low pressure limit to the rate constant is simply a constant. Since the rate of radiative emission is typically ~10^3 s^{-1}, this limit is not usually reached until very low pressures – e.g., ~10^{-6} bar. Nevertheless, in astrochemical environments the pressures are often much lower than that, and radiative emission is an important

process in that regime. Furthermore, such low pressures are accessible in current vacuum experiments, and it can be important to consider radiative processes. Indeed, some time ago, together with Dunbar,[51] we developed a scheme for employing a comparison of low-pressure ion-cyclotron resonance radiative association rate measurements with simple theoretical treatments to obtain estimated binding energies in ion-molecule complexes.

3.6 Multiple Exit Channels

As illustrated in a paper on dimethyl methane decomposition by Olzmann and coworkers for this discussion meeting, there can be many exit channels accessible from a single molecular species.[230] Furthermore, the branching between these channels can be a strong function of *E* and *J*, and thus *T* and *P*. For reactions with multiple exit channels, the branching to the higher channel can be exquisitely sensitive to the energy transfer parameters. For example, in C_2H_5OH there are two primary dissociation products: $C_2H_4 + H_2O$ and $CH_3 + CH_2OH$. The TS for the $C_2H_4 + H_2O$ channel lies 20 kcal mol^{-1} lower in energy that the $CH_3 + CH_2OH$ energy. Zhang and coworkers detailed uncertainty analysis of 1DME calculations for this system found a factor of 160 uncertainty in the rate to produce $CH_3 + CH_2OH$ at 1000 K and 0.001 atm.[231] Furthermore, this already very large uncertainty factor continues to increase with decreasing pressure and/or temperature.

The primary contributor to this uncertainty comes from the presumption of a 50% uncertainty in the $<\Delta E_{down}>$ value. In the low-pressure limit, production of $CH_3 + CH_2OH$ requires a collisional excitation of at least 20 kcal mol^{-1}. This level of excitation lies far into the tail of the collisional kernel $P(E, E')$. Clearly, the exponential down model is not designed to accurately treat the energy transfer probabilities that far into the tail. There is a strong need for more detailed comparisons of the temperature and pressure dependence of the product branching in reactions with multiple exit channels accessible. It is perhaps worth mentioning though that the probability of such events is low enough that the corresponding branching fraction is generally quite small, and thus usually not particularly important to the overall reaction rate. Nevertheless, this exquisite sensitivity does highlight the need for better understanding the limitations of the exponential down model coupled with the 1DME when considering branching fractions.

3.7 Multiple-Well Multiple-Channel (MWMC) Master Equation

For unimolecular reactions with multiple wells on the PES the *T* and *P* dependence of the decomposition kinetics can become remarkably complex due to the plethora of processes that exist and the complicated intermingling of their kinetics. The chemically significant eigenvalue (CSE) approach[17-19] provides an analytic one-to-one relation between the eigensolutions of the MWMC master equation and the phenomenological rate coefficients describing the time dependence of the species concentrations for all species for which a phenomenological rate description exists. Nevertheless, there are certain challenges that can arise when implementing the CSE approach.

In particular, at high *T* and/or low *P*, some of the eigenvalues that describe the chemical transitions can become of comparable magnitude to those that describe the intramolecular energy relaxation. Then, the presumed separation between chemical and relaxational eigenvalues, which provides the foundation for the CSE approach, begins to break down. In essence, a

phenomenological rate description for the corresponding eigenvalue simply ceases to exist. The isomerization of RO_2 and QOOH species provides a classic illustration of the conundrum provided by this rapid equilibration/merging of species. These two species typically merge near 600-800 K, which is exactly the region of interest to low *T* oxidation. Thus, at least for combustion chemistry, it is important to find solutions to this issue.

The formally correct solution to the issue is to realize that this merging of one of the CSEs into the quasi-continuum of relaxational eigenvalues correlates with the merging of two species into one. Those two species are now converting back and forth so rapidly that one cannot in any way isolate them kinetically within a thermal environment. Correspondingly, one should replace those two species with a single species within the phenomenological description. Within the master equation, the requisite state densities are then replaced with the union of the two independent densities (and similarly for the partition functions). Together with Miller we provided a detailed discussion of how such species merging is accomplished.[232] This species merging is performed automatically within MESS and depends only on a single parameter specifying at what point to consider a CSE to have merged into the quasicontinuum.

While formally this procedure provides the correct extension of the CSE approach to arbitrary conditions, it does create certain challenges for kinetic modeling. In particular, as one passes the temperature at which two species merge, there is a transition in the number of species. Standard kinetic modeling approaches do not allow for such a change in the kinetic representations. As a result, it is useful to continue to express the phenomenology in terms of the premerged list of species. To do so requires some approximate representation of the rate of transition between the two components of each merged pair of species.

We have recently developed a "well-extension" based approach for doing so through the introduction of artificially stabilized wells. This approach satisfies the following important set of conditions: First, the rate constants effectively coincide with the actual rate constants in their region of existence. Second, when species merge at higher temperatures and/or lower pressures, the extended rate constants are large enough to guarantee thermal equilibration within the combined species group. Last, but not least, the extended rate constants satisfy detailed balance. This approach is now integrated within the MESS software. An illustration of the approach for selected channels in the *n*-propyl RO_2/QOOH system is provided in Fig. 13. The solid lines denote the true phenomenological rate constants, while the

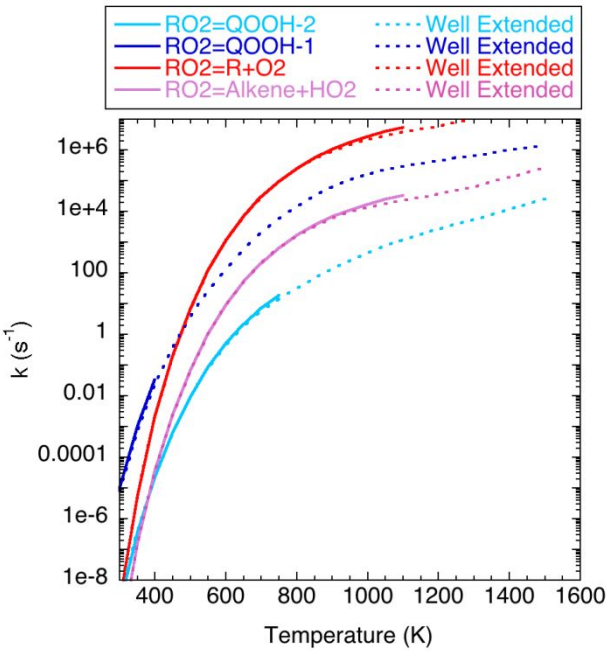

Fig. 13: The solid lines denote the phenomenological rate coefficients for the n-$C_3H_7O_2$ system, while the dotted lines denote their well-extended extrapolation to higher temperatures.

dashed lines illustrate our "well extension" based extrapolation of them to higher temperature.

A paper by Johnson and Green from this meeting discusses an alternative approach to extending the phenomenological description to cover all ranges of temperature and pressure.[34] It is based on the fitting of the full phenomenological rate description to the calculated time variation of the populations including the variation arising from the energy relaxation process. Johnson and Green perform this fitting for a specific set of initial conditions.

It is important to realize that no extended description of the phenomenological rate coefficients can be completely general. In particular, one cannot provide a description of both species in a merged pair of species that is correct for all initial conditions. Instead, the approach of Johnson and Green is specifically appropriate only for the presumed initial conditions of the fitting process. It should provide the correct rate description for the phenomenological rates that continue to exist, but for the other rates it is just providing an initial condition dependent prescription for the time variation. Meanwhile, the MESS approach simply provides an extrapolation of the rate coefficients for the independent components of the merged species that is physically appealing in its extrapolation. Likely, the two approaches yield similar results under most conditions.

Another approach to dealing with the merging issue is to instead artificially merge species even for temperatures where the relevant eigenvalue has not yet merged into the continuum. For large PAHs, with complex PESs, this approach has the desirable effect of significantly reducing the dimension of the fully phenomenological rate description. However, it does necessarily introduce some approximation. Such automated lumping procedures are also integrated within MESS. A recent paper from Pratali Maffei et al. provides an alternative post facto lumping based on species concentration fittings.[233]

At low temperatures the span in the eigenvalues can be very large, which creates numerical stability issues in the CSE approach. The temperature at which such problem occurs depends a lot on the system of interest, but it is not unusual to have troubles already at 800 K. The numerical issues are also particularly severe at lower P. Increasing the numerical precision employed in the eigensolver from double to quadruple or even octuple precision, as was first done in MESMER,[26,27] ameliorates such issues to some extent but issues still commonly arise. Furthermore, the calculations then become much more timeconsuming. The time to solution is an important concern in many cases, particularly for larger systems with many wells or when performing uncertainty and/or optimization studies. A much more effective approach to handling the numerical stability issues involves the use of a reservoir state,[234] which effectively amounts to replacing the detailed energy transitions at low energies to a Boltzmann distribution at a certain energy below the barrier. Within the reservoir state approach the connection between the high energy directly treated states and the low energy reservoir is done reversibly in a manner that maintains detailed balance. Within MESS we insert a reservoir state at some multiple of T (e.g., 10 k_BT) below the barrier, in contrast with traditional implementations that appear to employ reservoir states at a fixed E. This choice allows for numerically stable solutions to be obtained over very broad ranges of temperature for many situations, but some issues can still arise in MWMC cases. Although, solutions can generally be found on a case by case basis, further improvement in the numerical stability for the solutions would be valuable for automated kinetics approaches.

A study of Green et al. includes a nice comparison of various alternative, more approximate approaches, to solving the master equation.[235] In particular, the modified strong collider approach,[236] the reservoir state approach,[234] and the CSE approach are all compared.[17-19] The stochastic master equation approach provides another useful approach.[237] For complex reactions, the latter approach requires some sort of numerical inversion of the observed time dependent behavior back to the phenomenological rate coefficients.

For reactions of relevance to PAH formation, the web of wells and barriers connecting different species on the PES are often remarkably complex. Mebel has long been a leader in mapping such complex reactions. For this discussion meeting, Mebel and Frenklach provide PES mapping and kinetic studies for the dissociations of naphthalenyl, acetanaphthylenyl, and pyrenyl radicals.[238] The schematic diagram provided in Fig. 14 illustrates the complexity of such PESs for the interconnected dissociations of o-, m-, and p- xylyl (from ongoing work with Cavallotti, another leader in the field, and Georgievskii). The disparate well depths and barriers lead to a range of merging temperatures for the different pairs of species, as illustrated in Fig. 15.

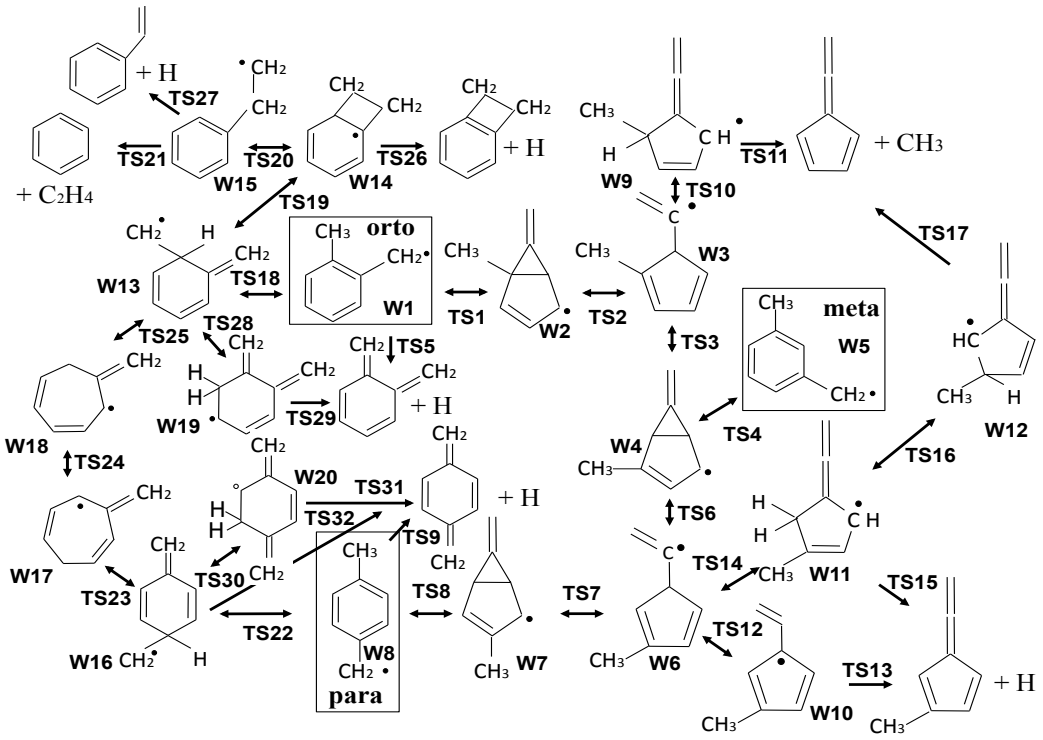

Fig. 14: Species connections on the PES for decomposition of Ortho (W1), Meta (W5), and Para (W8) C_8H_9.

The plot in Fig. 16 illustrates what we call the kinetic landscape for this system, i.e, the sequence of mergings that occur as the temperature is gradually increased from room temperature. It provides an informative picture of how the different species equilibrate. Panels a) to c) illustrate how the ortho, meta, and para wells are basins of attraction, with a number of other wells gradually getting merged into the ortho meta and para wells as the temperature is increased. Meanwhile, panel d) illustrates the temperature at which each of the remaining wells merge into various bimolecular products.

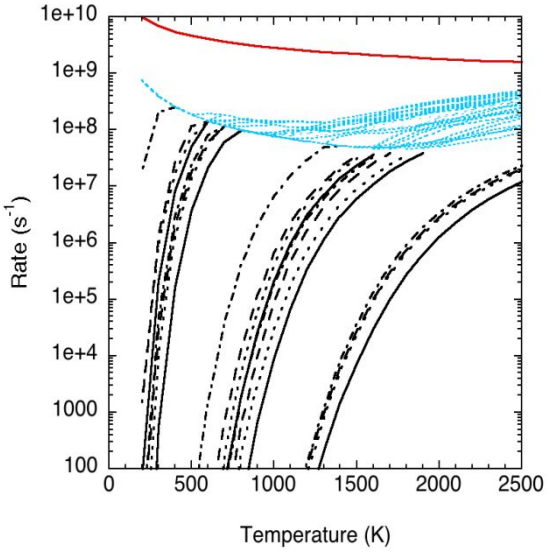

Fig. 15: Eigenvalue spectrum for C_8H_9 decomposition.

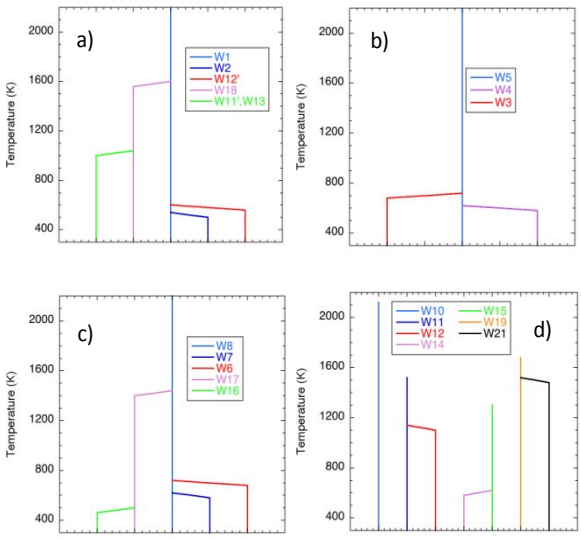

Fig. 16: Kinetic landscape plot for C_8H_9.

4. Automation

The implementation of the ab initio transition state theory based master equation (AI-TST-ME) methodology for an arbitrary unimolecular reaction involves some fairly tedious computational work. It requires the widespread application of ab initio electronic structure codes to find stationary points, energies, Hessians, and minimum energy paths for each of the reactive channels in the system. The information from these ab initio calculations must then be collected and prepared as input to a master equation code. The master equation codes must then be run over a range of *T* and *P* with the results then collected and fit to representations appropriate for use in chemical modeling. To further complicate matters, it is not uncommon for each of these steps to encounter some numerical difficulty.

The widespread recognition of the utility of AI-TST-ME calculations has led to a growing desire to increase the throughput of such studies. Thus, a number of groups have attempted to automate various aspects of these calculations, and recent years have seen great progress in that regard. Such efforts are non trivial due to the disparate nature of the various pieces, as well as the wide variety of ways in which the calculations can fail. An excellent review of the current status of these efforts has recently been provided by Cavallotti.[239] We provide here only a brief mention of some of the more substantive efforts.

There are now a variety of approaches that focus primarily on the mapping of the PES, as recently reviewed by Unsleber and Reiher.[240] In the artificial force induced mapping method of Maeda et al.[241] the saddle points from a given potential energy minima are found by considering a set of fragmentation possibilities. The AFIR method is quite unique, and appears to be highly successful as judged from its diverse set of applications. With the KinBot code of Van de Vivjer and Zador,[242] a set of saddle points are instead determined according to a predefined set of reaction classes. String based methods (e.g., the growing string method, GSM, and the single-ended

growing string method SSM) are also popular.[243,244] Other approaches, such as the ChemTraYZer approach of Leonhard and coworkers[245,246] and the AutoMeKin2021 code of Martinez and coworkers[247] instead employ molecular dynamics simulations in the initial saddle point discovery. A recent study provided an informative comparison of the AFIR, GSM, SSM, and KinBot methods.[248] This comparison was later updated with a more careful implementation of the AFIR code.[249] There are advantages and disadvantages to these various approaches, and to the particular implementations of them that are readily available. To a great degree, the optimal method is highly dependent on the purpose of the analysis.

For cases where the reaction mechanism is known, as is often the case, and the user just wishes to find a particular saddle point connecting a prespecified reactant and product, then simpler reaction specific approaches are useful. Truhlar and coworkers combination of Polyrate[67] and Gaussrate[250] codes provided some of the earliest examples of coupling ab initio potential energy surface mapping with transition state analyses. These codes remain the most effective schemes for implementing variational TST. West and coworkers developed the AutoTST code[251] to find saddle points and implement TST for abstraction, hydrogen migration, and radical addition reactions via group libraries of initial guesses for the saddle point geometries.

The EStokTP code of Cavallotti and coworkers for the first time provided a full and direct coupling of PES mapping, variational transition state theory, and torsional analyses with the MESS master equation code. Initially, the PES mapping was limited to abstraction, addition, beta-scission, and isomerization reaction, but that list has been expanded. The code uses simple generic templates for each of the reaction classes. These templates use a limited set of constrained optimizations to obtain high quality starting guesses for the saddle point geometries. The use of generic prescriptions facilitates the implementation of the code for a wide variety of reactions within the generic reaction classes. The TS searching algorithm was shown to have a remarkably high success rate (> 95%) in its initial testing, [252] which is a key prerequisite to performing fully automated large scale kinetic mappings. The code was designed to automate all aspects of high level AI-TST-ME evaluations. It included conformational sampling, multidimensional torsional mapping, high level energies, symmetry number evaluations, and variational TST implementations (including a recent extension by Cavallotti to include VRC-TST).

The success and utility of the EStokTP code led us to embark on a grander vision of developing a code that could take a given mechanism for some complex reactive environment and produce first principles theoretical predictions for all of the underlying kinetic, thermodynamic, and transport properties. Implementing this vision turned out to be quite a challenge, requiring deep dives into cheminformatics, graph theory, file management and databasing, improvements in our TS searching and mapping protocols, and further automation of the procedures for converting from master equation solutions to phenomenological representations. The end product of this effort is the AutoMech software suite,[107,108] which can be viewed as the logical extension of the EStokTP code from single reactions to a whole mechanism. Nevertheless, the EStokTP code itself retains great utility in its simpler focus on single reactions. Some recent publications demonstrate some of the capabilities of the AutoMech code,[138,253,254] but many more are now available, and we continue to work at expanding its utility in a variety of ways.

It is perhaps worth noting that the Green group has recently tackled many of the same issues in their development of the Arkane software.[255] More importantly, we should note that other theoretical kineticists, such as Vereecken, are prolific enough in their computations, that it is clear that they must have their own self-contained automation efforts. It is exciting to see how greatly the throughput and the quality of theoretical calculations for unimolecular reaction kinetics has increased in recent years.

5. Conclusion

Recent years have seen spectacular progress in our ability to measure, interpret, and predict the kinetics and dynamics of unimolecular reactions. This understanding arises from the long and concerted effort to connect theory and experiment for ever more complex reactions and reactive systems. Building from the foundational perspective provided by first the Lindemann mechanism and then RRKM theory with its explicit statistical theory prescriptions, the master equation now provides the basis for essentially all theoretical kinetics analyses. One notable finding is that careful attention to details (e.g., tunneling, competing channels, non-thermal effects including reactive depletion of Boltzmann distributions, radiative emission, and the effect of long-range complexes) indicates significant deviations from the classic pressure dependence of the Lindemann mechanism (linear in P at low pressures and independent of P in the high pressure limit). They also indicate some pressure dependence where none was previously expected.

Remarkably, all components of the master equation can now often be evaluated to a high degree of accuracy with first principles theory through couplings of ab initio electronic structure and dynamics calculations (although inadequate utilization of existing theoretical methodology still limits many studies). Nevertheless, there are still many important frontiers for furthering our understanding. There is a need for continued experimental examination of complex reactions, especially for highly transient species, for ones leading to the formation of multiple products, and to examine the effect of processes occurring in the long-range region of the potential energy surface. The theoretical prescriptions for calculating the rate coefficients need to progress to the point that high accuracy predictions are readily obtained even for large molecules and for reactions occurring over complex potential energy systems. Further studies and methods for treating collisional E and J transfer kernels, anharmonic effects, intersystem crossing, tunneling, dynamics on the long-range/roaming region of the potentials, as well as for hot reactants, are all warranted.

One repeated finding over the last few years is that in complex reactive environments reactions often do not occur as isolated reactions of thermalized species. Instead, the distribution of energy states that the molecule is prepared in can have significant ramifications for the overall chemistry of the system. Because of this, it is becoming increasingly important to replace the standard single reaction master equation simulations with ones that describe a whole sequence of non-thermal events. For the simple prompt dissociation sequence, this coupling of reactions is readily achieved and has now been implemented in freely available software. For limited sequences of bimolecular reactions, some progress has been made, but certain approximations are being made, and it is difficult to know how far back in the reaction system one should couple the reactions. I believe that ultimately some form of complete/global master equation modeling, where the energy populations of essentially all of the species are propagated together in time, will be used to definitively explore the ramifications of non-thermal effects in chemically reactive systems. For

simple systems, such as the H_2 oxidation environment, it is clear that such complete master equation modeling is now technically feasible. Such global master equation modeling would provide the first fully in silico high accuracy modeling of a complex reactive environment.

Acknowledgements

This material is based on work supported by the U.S. Department of Energy, Office of Science, Office of Basic Energy Sciences, Division of Chemical Sciences, Geosciences, and Biosciences under contract No. DE-AC02-06CH11357. I am also indebted to my numerous cited collaborators, who have each been instrumental in advancing our knowledge of unimolecular reactions.

References:

[1] F. A. Lindemann, Discussion on the Radiation Theory of Chemical Action, *Trans. Faraday Soc.,* 1922, **17,** 598-606.
[2] R. A. Marcus, Unimolecular Dissociation and Free Radical Recombination Reactions, *J. Chem. Phys.,* 1954, **20**, 359-364.
[3] K. A. Holbrook, M. J. Pilling, S. H. Robertson, Unimolecular Reactions, 2nd Ed. John Wiley, Chichester, 1996.
[4] D. G. Truhlar, B. C. Garrett, S. J. Klippenstein, Current Status of Transition Theory, *J. Phys. Chem*. 1996, **100**, 12771-12800.
[5] L. D. Spicer, B. S. Rabinovitch, Elementary Gas Reactions, *Annu. Rev. Phys. Chem*. 1970, **21**, 349-386.
[6] R. G. Gilbert, S. C. Smith, Theory of Unimolecular and Recombination Reactions, Blackwell, Oxford, 1990.
[7] J. Troe, Theory of Thermal Unimolecular Reactions at Low-Pressures. 1. Solutions of Master Equation, *J. Chem. Phys.* 1977, **66**, 4745-4757.
[8] R. G. Gilbert, K. Luther, J. Troe, Theory of Thermal Unimolecular Reactions in the Fall-Off Range. 2. Weak Collision Rate Constants, *Ber. Buns. Ges. Phys. Chem. Chem. Phys.* 1983, **87**, 169-177.
[9] J. Troe, Predictive Possibilities of Unimolecular Rate Theory, *J. Phys. Chem.* 1979, **83**, 114-126.
[10] J. A. Miller, C. F. Melius, Kinetic and Thermodynamic Issues in the Formation of Aromatic-Compounds in Flames of Aliphatic Fuels, *Combust. Flame*, 1992, **91**, 21-39.
[11] S. J. Klippenstein, Variational Optimizations in the Rice-Ramsperger-Kassel-Marcus Theory Calculations for Unimolecular Dissociations with No Reverse Barrier, *J. Chem. Phys*. 1992, **96**, 367-371.
[12] S. J. Klippenstein, A. F. Wagner, R. C. Dunbar, D. M. Wardlaw, S. H. Robertson, VariFlex Version 1.00, 1999.
[13] K. E. Gates, S. H. Robertson, S. C. Smith, M. J. Pilling, M. S. Beasley, K. J. Maschhoff, Multiple-Well Isomerization Diffusion Equation Solutions with a Shift and Invert Lanczos Algorithm, *J. Phys. Chem. A*, 1997, **101**, 5765-5769.
[14] J. A. Miller, S. J. Klippenstein, S. H. Robertson, A Theoretical Analysis of the Reaction between Vinyl and Acetylene: Quantum Chemistry and Solution of the Master Equation, *J. Phys. Chem. A*, 2000, **104**, 7525-7536.
[15] J. A. Miller, S. J. Klippenstein, S. H. Robertson, A Theoretical Analysis of the Reaction Between Ethyl and Molecular Oxygen, *Proc. Combust. Inst.* 2000, **28**, 1479-1486.
[16] J. D. DeSain, S. J. Klippenstein, J. A. Miller, C. A. Taatjes, Measurements, Theory, and Modeling of OH Formation in Ethyl + O_2 and Propyl + O_2 Reactions, J. Phys. Chem. A, 2003, **107**, 4415-4427.
[17] S. J. Klippenstein, J. A. Miller, From the Time-Dependent, Multiple-Well Master Equation to Phenomenological Rate Coefficients, *J. Phys. Chem. A* 2002, **106**, 9267-9277.
[18] J. A. Miller, S. J. Klippenstein, From the Multiple-Well Master Equation to Phenomenological Rate Coefficients: Reactions on a C_3H_4 Potential Energy Surface, *J. Phys. Chem. A* 2003, **107**, 2680-2692.
[19] J. A. Miller, S. J. Klippenstein, Master Equation Method in Gas Phase Chemical Kinetics, *J. Phys. Chem. A*, 2006, **110**, 10528-10544.
[20] J. T. Bartis, B. Widom, Stochastic Models of the Interconversion of Three or More Chemical Species, *J. Chem. Phys.* 1974, **60**, 3474-3482.
[21] J. A. Miller, S. J. Klippenstein, The Recombination of Propargyl Radicals and Other Reactions on a C_6H_6 Potential, *J. Phys. Chem. A*, 2003, **107**, 7783-7799.
[22] J. D. Savee, B. Sztaray, P. Hemberger, J. Zador, A. Bodi, D. L. Osborn, Unimolecular Isomerisation of 1,5-Hexadiyne Observed by Threshold Photoelectron Photoion Coincidence Spectroscopy, *Faraday Disc*. 2022, in press.
[23] M. Jarraya, A. Bellili, L. Barreau, D. Cubaynes, G. A. Garcia, L. Poisson, M. Hochlaf, Probing the Dynamics of the Photo-Induced Decarboxylation of Neutral and Ionic Pyruvic Acid, *Faraday Disc*. 2022, in press.
[24] Y. Georgievskii, J. A. Miller, S. J. Klippenstein, Association Rate Constants for Reactions Between Resonance-Stabilized Radicals: C_3H_3 + C_3H_3, C_3H_3 + C_3H_5, and C_3H_5 + C_3H_5, *Phys. Chem. Chem. Phys.* 2007, **9**, 4259-4268.
[25] A. I. Maergoiz, E. E. Nikitin, J. Troe, Statistical Theory for the Reaction N + OH $\rightarrow$ NO + H Thermal Low-Temperature Rate Constants, *Faraday Disc*. 2022, in press.
[26] D. R. Glowacki, C.-H. Liang, C. Morley, M. J. Pilling, S. H. Robertson, MESMER: An Open-Source Master Equation Solver for Multi-Energy Well Reactions, *J. Phys. Chem. A,* 2012, **116**, 9545-9560.
[27] https://sourceforge.net/projects/mesmer/
[28] R. M. Zhang, X. F. Xu, D. G. Truhlar, TUMME: Tsinghua University Minnesota Master Equation Program, *Comp. Phys. Comm*. 2022, **270**, 108140.
[29] https://comp.chem.umn.edu/tumme/
[30] Y. Georgievskii, J. A. Miller, M. P. Burke, S. J. Klippenstein, Reformulation and Solution of the Master Equation for Multiple-Well Chemical Reactions, *J. Phys. Chem. A*, 2013, **117**, 12146-12154.

[31] https://github.com/Auto-Mech/MESS. Master Equation System Solver calculates temperature and pressure dependent rate coefficients for complex-forming reactions via solution of the one-dimensional master equation.
[32] J. R. Barker, Multiple-Well, Multiple-Path Unimolecular Reaction Systems. I. MultiWell Computer Program Suite, Int. J. Chem. Kinet. 2001, 33, 232-245.
[33] https://clasp-research.engin.umich.edu/multiwell/
[34] M. S. Johnson, W. H. Green, Examining the Accuracy of Methods for Obtaining Pressure Dependent Rate Coefficients, *Faraday Disc.* 2022, in press.
[35] H. Hippler, K. Luther, J. Troe, J. Wendelken, Unimolecular Processes in Vibrationally Highly Excited Cycloheptatrienes. 3. Direc k(E) Measurements After Laser Excitation, *J. Chem. Phys.* 1983, **79**, 239-246
[36] L. R. Khundkar, J. L. Knee, A. H. Zewail, Picosecond Photofragment Spectroscopy. 1. Microcanonical State-to-State Rates of the Reaction NCNO → CN + NO, *J. Chem. Phys.* 1987, **87**, 77-96.
[37] S. J. Klippenstein, L. R. Khundkar, A. H. Zewail, R. A. Marcus, Application of Unimolecular Reaction-Rate Theory for Highly Flexible Transition-States to the Dissociation of NCNO into NC and NO, *J. Chem. Phys.* 1988, 89 4761-4770.
[38] E. D. Potter, M. Gruebele, L. R. Khundkar, A. H. Zewail, Picosecond Dissociation of Ketene – Experimental State-to-State Rates and Tests of Statistical Theories, *Chem. Phys. Letts*. 1989, **164**, 463-470.
[39] S. K. Kim, Y. S. Choi, C. D. Pibel, Q.-K. Zheng, C. B. Moore, Determination of the Singlet Triplet Branching Ratio in the Photodissociation of Ketene, *J. Chem. Phys*. 1991, **94**, 1954-1960.
[40] S. J. Klippenstein, R. A. Marcus, Application of Unimolecular Reaction-Rate Theory for Highly Flexible Transition-States to the Dissociation of CH_2CO into CH_2 and CO, *J. Chem. Phys*. 1989, **91**, 2280-292.
[41] S. J. Klippenstein, A. L. L. East, W. D. Allen, A First Principles Theoretical Determination of the Rate-Constant for the Dissociation of Singlet Ketene, *J. Chem. Phys.* 1994, **101**, 9198-9201.
[42] J. W. Yu, S. J. Klippenstein, Variational Calculation of the Rate of Dissociation of CH_2CO into $^1CH_2$ and CO on an Ab Initio Determined Potential-Energy Surface, *J. Phys. Chem.* 1991, **95**, 9882-9889.
[43] S. J. Klippenstein, A. L. L. East, W. D. Allen, A High Level Ab Initio Map and Direct Statistical Treatment of the Fragmentation of Singlet Ketene, *J. Chem. Phys.* 1996, **105**, 118-140.
[44] C. B. Moore, J. C. Weishaar, Formaldehyde Photochemistry, *Ann. Rev. Phys. Chem.* 1983, **34**, 525-555.
[45] G. A. Brucker, S. I. Ionov, Y. Chen, C. Wittig, Time-Resolved Studies of NO_2 Photoinitiated Unimolecular Decomposition: Step-Like Variation of $k_{uni}(E)$, *Chem. Phys. Lett.* 1992, **194**, 301-308.
[46] I. Bezel, P. Ionov, C. Wittig, Photoinitiated Unimolecular Dissociation of NO_2: Rotational Dependence of the Dissociation Rate, *J. Chem. Phys*. 1999, **111**, 9267-9279.
[47] S. J. Klippenstein, T. Radivoyevitch, A Theoretical Study of the Dissociation of NO_2, *J. Chem. Phys.* 1993, **99**, 3644-3653.
[48] F. F. Crim, Selective Excitation Studies of Unimolecular Reaction Dynamics, *Annu. Rev. Phys. Chem*. 1984, **35**, 657-691.
[49] B. Sztaray, A. Bodi, T. Baer, Modeling Unimolecular Reactions in Photoelectron Photoion Coincidence Experiments, *J. Mass. Spec*. 2010, **45**, 1233-1245.
[50] S. J. Klippenstein, J. D. Faulk, R. C. Dunbar, A Combined Theoretical and Experimental Study of the Dissociation of Benzene Cation, *J. Chem. Phys*. 1993, **98**, 243-256.
[51] S. J. Klippenstein, Y. C. Yang, R. C. Dunbar, Theory and Modeling of Ion-Molecule Radiative Association Kinetics, *J. Chem. Phys.* 1996, **104**, 4502-4516.
[52] M. T. Rodgers, K. M. Ervin, P. B. Armentrout, Statistical Modeling of Collision-Induced Dissociation Thresholds, *J. Chem. Phys*. 1997, **106**, 4499-4508.
[53] M. T. Rodgers, P. B. Armentrout, Statistical Modeling of Competetive Threshold Collision-Induced Dissociation, *J. Chem. Phys*. 1998, **109**, 1787
[54] O. J. Shiels, J. A. Turner, P. D. Kelly, S. J. Blanksby, G. da Silva, A. J. Trevitt, Modelling Reaction Kinetics of Distonic Radical Ions: A Systematic Investigation of Phenyl-Type Radical Addition to Unsaturated Hydrocarbons, *Faraday Disc*. 2022, in press.
[55] D. Heathcote, P. A. Robertson, A. A. Butler, C. Ridley, J. Lomas, M. M. Buffett, M. Bell, C. Vallance, Electron-Induced Dissociation Dynamics Studied Using Covariance-Map Imaging, *Faraday Disc*. 2022, in press.
[56] Y. Fang, F. Liu, V. P. Barber, S. J. Klippenstein, A. B. McCoy, M. I. Lester, Communcation: Real Time Observation of Unimolecular Decay of Criegee Intermediates to OH Radical Products, *J. Chem. Phys*. 2016, **144**, 061102.
[57] M. I. Lester, S. J. Klippenstein, Unimolecular Decay of Criegee Intermediates to OH Radical Products: Prompt and Thermal Decay Processes, *Acc. Chem. Res*. 2018, **51**, 978−985.

[58] T. T. Pekkanen, R. S. Timonen, S. H. Robertson, G. Lendvay, S. P. Joshi, T. T. Reigonen, A. J. Eskola, An Experimental and Computational Study of the Reaction Between 2-Methylallyl Radicals and Oxygen Molecules: Optimizing Master Equation Parameters with Trace Fitting, *Phys. Chem. Chem. Phys.* 2022, **24**, 4729-4742.
[59] T. T. Pekkanen, L. Valkai, S. P. Joshi, G. Lendvay, P. Heinonen, R. S. Timonen, A. J. Eskola, An Experimental and Computational Study of the Reaction Between Pent-3-en-2-yl Radicals and Oxygen Molecules: Switching from Pure Stabilisation to Pure Decomposition with Increasing Temperature, *Faraday Disc.* 2022, in press.
[60] A. S. Hansen, T. Bhagde, K. B. Moore III, D. R. Moberg, A. W. Jasper, Y. Georgievskii, M. F. Vansco, S. J. Klippenstein, M. I. Lester, Watching a Hydroperoxyalkyl Radical (•QOOH) Dissociate, *Science*, 2021, **373**, 679-682.
[61] T. Bhagde, A. S. Hansen, S. Chen, P. J. Walsh, S. J. Klippenstein, M. I. Lester, Energy-Resolved and Time-Dependent Unimolecular Dissociation of Hydroperoxyalkyl Radicals (•QOOH), *Faraday Disc.* 2022, in press.
[62] C. Eckart, The Penetration of a Potential Barrier by Electrons, *Phys. Rev*. 1930, **35**, 1303-1309.
[63] R. T. Skodje, D. G. Truhlar, B. C. Garrett, A General Small-Curvature Approximation of Transition-State-Theory Transmission Coefficients, *J. Phys. Chem.* 1981, **85**, 3019-3023.
[64] R. T. Skodje, D. G. Truhlar, B. C. Garrett, Vibrationally Adiabatic Models for Reactive Tunneling, *J. Chem. Phys.* 1982, **77**, 5955-5976.
[65] A. Fernandez-Ramos, D. G. Truhlar, A New Algorithm for Efficient Direct Dynamics Calculations of Large-Curvature Tunneling and Its Application ot Radical Reactions with 9-14 Atoms, *J. Chem. Theory Comput*. 2005, **1**, 1063-1078.
[66] R. Meana-Paneda, D. G. Truhlar, A. Fernandez-Ramos, Least Action Tunneling Transmission Coefficient for Polyatomic Reactions, *J. Chem. Theory Comput*. 2010, **6**, 6-17.
[67] https://comp.chem.umn.edu/polyrate/ Polyrate 17-C: Computer Program for the Calculation of Chemical Reaction Rates for Polyatomics.
[68] W. H. Miller, R. Hernandez, N. C. Handy, D. Jayatilaka, A. Willetts, Ab Initio Calculation of Anharmonic Constants for a Transition State, with Application to Semiclassical Transition State Tunneling Probabilities, *Chem. Phys. Lett.* 1990, **172**, 62-68.
[69] R. E. Weston, T. L. Nguyen, J. F. Stanton, J. R. Barker, HO + CO Reaction Rates and H/D Kinetic Isotope Effects: Master Equation Models with Ab Initio SCTST Rate Constants, *J. Phys. Chem. A*, 2013, **117**, 821-835.
[70] J. R. Barker, J. F. Stanton, T. L. Nguyen, Semiclassical Transition State Theory/Master Equation Kinetics of HO + CO: Performance Evaluation, *Int. J. Chem. Kinet*. 2020, **52**, 1022-1045.
[71] T. L. Nguyen, D. H. Bross, B. Ruscic, G. B. Ellison, J. F. Stanton, Mechanism, Thermochemistry, and Kinetics of the Reversible Reactions: $C_2H_3 + H_2 = C_2H_4 + H = C_2H_5$, *Faraday Disc.* 2022, in press.
[72] D. C. Clary, Introductory Lecture: Quantum Dynamics of Chemical Reactions, *Faraday Disc*. 2018, **212**, 9-32.
[73] A. F. Wagner, Improved Multidimensional Semiclassical Tunneling Theory, *J. Phys. Chem. A*, 2013, **117**, 13089-13100.
[74] Y. Georgievskii, S. J. Klippenstein, Entanglement Effect and Angular Momentum Conservation in a Nonseparable Tunneling Treatment, *J. Chem. Theory Comput*. 2021, **17**, 3863-3885.
[75] L.A. Curtiss, P.C. Redfern, K. Raghavachari, Gaussian-4 Theory, *J. Chem. Phys.* 2007, **126**, 084108.
[76] J.A. Montgomery, M.J. Frisch, J.W. Ochterski, G.A. Petersson, A Complete Basis Set Model Chemistry. VI. Use of Density Functional Geometries and Frequencies, *J. Chem. Phys*. 1999, **110**, 2822-2827.
[77] S.J. Klippenstein, L.B. Harding, B. Ruscic, Ab Initio Computations and Active Tables Hand in Hand: Heats of Formation of Core Combustion Species, *J. Phys. Chem. A* 2017, **121**, 6580-6602.
[78] G. Knizia, T.B. Adler, H.-J. Werner, Simplified CCSD(T)-F12 Methods: Theory and Benchmarks, *J. Chem. Phys*. 2009, **130**, 054104.
[79] M. Saltow, U. Becker, C. Riplinger, E. F. Valeev, F. Neese, A New Near-Linear Scaling Efficient and Accurate, Open-Shell Domain-Based Local Pair Natural Orbital Coupled Cluster Singles and Doubles Theory, *J. Chem. Phys.* 2017, **146**, 164105
[80] E. Paulechka, A. Kazakov, Efficient DLPNO-CCSD(T)-Based Estimation of Formation Enthalpies for C-, H-, O-, and N-Containing Closed-Shell Compounds Validated Against Critically Evaluated Experimental Data, *J. Phys. Chem. A* 2017, **121**, 4379-4387.
[81] Q. Ma, H.-J. Werner, Explicitly Correlated Local Coupled-Cluster Methods Using Pair Natural Orbitals, *WIRES: Comp. Mol. Sci.* 2018, **8**, e1371.
[82] F. Neese, Software Update: The ORCA Program System, Version 4.0, *WIREs: Comp. Mol.* Sci. 2018, **8**, e1327.
[83] MOLPRO, version 2022.1.1, a package of ab initio programs, H.-J. Werner, P. J. Knowles, G. Knizia, F. R. Manby, M. Schütz, P. Celani, W. Györffy, D. Kats, T. Korona, R. Lindh, A. Mitrushenkov, G. Rauhut, K. R. Shamasundar, T. B. Adler, R. D. Amos, S. J. Bennie, A. Bernhardsson, A. Berning, D. L. Cooper, M. J. O. Deegan, A. J. Dobbyn,

F. Eckert, E. Goll, C. Hampel, A. Hesselmann, G. Hetzer, T. Hrenar, G. Jansen, C. Köppl, S. J. R. Lee, Y. Liu, A. W. Lloyd, Q. Ma, R. A. Mata, A. J. May, S. J. McNicholas, W. Meyer, T. F. Miller III, M. E. Mura, A. Nicklass, D. P. O'Neill, P. Palmieri, D. Peng, T. Petrenko, K. Pflüger, R. Pitzer, M. Reiher, T. Shiozaki, H. Stoll, A. J. Stone, R. Tarroni, T. Thorsteinsson, M. Wang, and M. Welborn, see http://www.molpro.net

[84] H. J. Werner, P. J. Knowles, F. R. Manby, J. A. Black, K. Doll, A. Heßelmann, D. Kats, A. Köhn, T. Korona, David A. Kreplin, Q. Ma, T. F. Miller, III, A.r Mitrushchenkov, K.A. Peterson, I. Polyak, G. Rauhut, M. Sibaev, The Molpro Quantum Chemistry Package, *J. Chem. Phys*. 2020, **152**, 144107.

[85] A. Karton, E. Rabinovitch, J. M. L. Martin, B. Ruscic, W4 Theory for Computational Thermochemistry: In Pursuit of Confident sub-kJ/mol Predictions, *J. Chem. Phys*. 2006, **125**, 144108.

[86] M. E. Harding, J. Vazquez, B. Ruscic, A. K. Wilson, J. Gauss, J. F. Stanton, High-Accuracy Extrapolated Ab Initio Thermochemistry. III. Additional Improvements and Overview, *J. Chem. Phys*. 2008, **128**, 114111.

[87] H. M. Schaefer, H. F. Schaefer, J. Demaison, A. G. Csaszar, W. D. Allen, Lowest-Lying Conformers of Alanine: Pushing Theory to Ascertain Precise Energetics and Semiexperimental Re Structures, *J. Chem. Theory Comput*. 2010, **6**, 3066-3078.

[88] K. A. Peterson, D. Feller, D. A. Dixon, Chemical Accuracy in Ab Initio Thermochemistry and Spectroscopy: Current Strategies and Future Challenges, *Theor. Chem. Acc*. 2012, **131**, 1079-1099.

[89] B. Ruscic, R. E. Pinzon, M. L. Morton, G. von Laszewski, S. J. Bittner, S. G. Nijsure, K. A. Amin, M. Minkoff, A. F. Wagner, Introduction to Active Thermochemical Tables: Several "Key" Enthalpies of Formation Revisited, *J. Phys. Chem. A* 2004, **108**, 9979-9997.

[90] B. Ruscic, R. E. Pinzon, G. von Laszewski, D. Kodeboyina, A. Burcat, D. Leahy, A. F. Wagner, Active Thermochemical Tables: Thermochemistry for the 21st Century, *J. Phys. Conf. Ser*. 2005, **16**, 561-570.

[91] https://atct.anl.gov/Thermochemical%20Data/version%201.122p/index.php; Active Thermochemical Tables.

[92] S. Grimme, Semiempirical Hybrid Density Functional with Perturbative Second-Order Correlation, *J. Chem. Phys*. 2006, **124**, 034108.

[93] G. Santra, N. Sylvetsky, J. M. L. Martin, Minimally Empirical Double-Hybrid Functionals Trained against the GMTKN55 Database: revDSD-PBEP86-D4, revDOD-PBE-D4, and DOD-SCAN-D4, *J. Phys. Chem. A* 2019, **123**, 5129-5143.

[94] J. Bloino, M. Biczysko, V. Barone, General Perturbative Approach for Spectroscopy, Thermodynamics, and Kinetics: Methodological Background and Benchmark Studies, *J. Chem. Theory Comput*. 2012, **8**, 1015−1036.

[95] L. B. Harding, Y. Georgievskii, S. J. Klippenstein, Accurate Anharmonic Zero-Point Energies for some Combustion-Related Species from Diffusion Monte Carlo, *J. Phys. Chem. A*, 2017, **121**, 4334-4340.

[96] B. Chan, L. Radom, W2X and W3X-L: Cost-Effective Approximations to W2 and W4 with kJ mol^{-1} Accuracy, *J. Chem. Theory Comput.* 2015, **11**, 2109-2119.

[97] A. Ganyecz, M. Kallay, J. Csontos, Moderate-Cost Ab Initio Thermochemistry with Chemical Accuracy, *J. Chem. Theory Comput.* 2017, **13**, 4193-4204.

[98] J. H. Thorpe, C. A. Lopez, T. L. Nguyen, J. H. Baraban, D. H. Bross, B. Ruscic, J. F. Stanton, *J. Chem. Phys.* 2019, **150**, 224102.

[99] Y. Zhao, L. Xia, X. Liao, Q. He, M. X. Zhao, D. G. Truhlar, Extrapolation of High-Order Correlation Energies: The WMS Model, *Phys. Chem. Chem. Phys*. 2018, **20**, 27375-27384.

[100] C.F. Melius, J.S. Binkley, Thermochemistry of the Decomposition of Nitramines in the Gas Phase, *Proc. Combust. Inst.* 1986, **21**, 1953–1963.

[101] C.F. Goldsmith, G.R. Magoon, W.H. Green, Database of Small Molecule Thermochemistry for Combustion, *J. Phys. Chem. A* 2012, **116**, 9033–9057.

[102] S. E. Wheeler, K. N. Houk, P. v. R. Schleyer, W. D. Allen, A Hierarchy of Homodesmotic Reactions for Thermochemistry, *J. Am. Chem. Soc*. 2009, **131**, 2547-2560.

[103] J. M. Simmie, K. P. Somers, W. K. Metcalfe, H. J. Curran, Substituent Effects in the Thermochemistry of Furans: A Theoretical (CBS-QB3, CBS-APNO, and G3) Study, *J. Chem. Thermo.* 2013, **58**, 117-128.

[104] R. O. Ramabhadran, K. Raghavachari, Theoretical Thermochemistry for Organic Molecules: Development of the Generalized Connectivity-Based Hierarchy, *J. Chem. Theory Comput.* 2011, **7**, 2094–2103.

[105] R. O. Ramabhadran, K. Raghavachari, Connectivity-Based Hierarchy for Theoretical Thermochemistry: Assessment Using Wave Function-Based Methods, *J. Phys. Chem. A* 2012, **116**, 7531–7537.

[106] A. Sengupta, K. Raghavachari, Prediction of Accurate Thermochemistry of Medium and Large Sized Radicals Using Connectivity-Based Hierarchy (CBH), *J. Chem. Theory Comput.* 2014, **10**, 4342–4350.

[107] https://tcg.cse.anl.gov/papr/codes/automech.html

[108] https://github.com/Auto-Mech; Computes and databased high-accuracy quantum chemistry, thermochemistry, and kinetic data via automated workflows to improve chemical mechanism models.
[109] S. N. Elliott, S. J. Klippenstein, work in progress.
[110] V. D. Knyazev, Reactivity Extrapolation from Small to Large Molecular Systems via Isodesmic Reactions for Transition States, *J. Phys. Chem. A*, 2004, **108**, 10714-10722
[111] A. Karton, Highly Accurate CCSDT(Q)/CBS Reaction Barrier Heights for a Diverse Set of Transition Structures: Basis Set Convergence and Cost-Effective Approaches for Estimating Post-CCSD(T) Contributions, *J. Phys. Chem. A,* 2019, **123**, 6720-6732.
[112] A. W. Jasper, L. B. Harding, C. Knight, Y. Georgievskii, Anharmonic Rovibrational Partition Functions at High Temperatures: Tests of Reduced-Dimensional Models for Systems with up to Three Fluxional Modes, *J. Phys. Chem. A*, 2019, **123**, 6210-6228.
[113] A. W. Jasper, Z. B. Gruey, L. B. Harding, Y. Georgievskii, S. J. Klippenstein, A. F. Wagner, Anharmonic Rovibrational Partition Functions for Fluxional Species at High Temperatures via Monte Carlo Phase Space Integrals, *J. Phys. Chem. A*, 2018, **122**, 1727-1740.
[114] D. Ferro-Costas, M. N. D. S. Cordeiro, D. G. Truhlar, A. Fernandez-Ramos, Q2DTor: A Program to Treat Torsional Anharmonicity through Coupled Pair Torsions in Flexible Molecules, *Comp. Phys. Comm*. 2018, **232**, 190-205.
[115] V. P. Barber, A. S. Hansen, Y. Georgievskii, S. J. Klippenstein, M. I. Lester, Experimental and Theoretical Studies of the Double Substituted Methyl Ethyl Criegee Intermediate: Infrared Action Spectroscopy and Unimolecular Decay to OH Radical Products, *J. Chem. Phys*. 2020, **152**, 094301.
[116] L. Vereecken, J. Peeters, The 1,5-H-Shift in 1-Butoxy: A Case Study in the Rigorous Implementation of Transition State Theory for a Multirotamer System, *J. Chem. Phys.* 2003, **119**, 5159-5170.
[117] A. S. Petit, J. N. Harvey, Atmospheric Hydrocarbon Activation by the Hydroxyl Radical: A Simple Yet Accurate Computational Protocol for Calculating Rate Coefficients, *Phys. Chem. Chem. Phys*. 2012, **14**, 184-191.
[118] J. Zheng, S. L. Mielke, K. L. Clarkson, D. G. Truhlar, MSTor: A Program for Calculating Partition Functions, Free Energies, Enthalpies, and Heat Capacities of Complex Molecules Including Torsional Anharmonicity, *Comp. Phys. Comm.* 2012, **183**, 1803-1812.
[119] J. L. Bao, L. Xing, D. G. Truhlar, Dual-Level Method for Estimating Multistructural Partition Functions with Torsional Anharmonicity, *J. Chem. Theory Comput.* 2017, **13**, 2511-2522.
[120] J. J. Zheng, R. Meana-Paneda, D. G. Truhlar, MSTor Version 2013: A New Version of the Computer Code for the Multi-Structural Torsional Anharmonicity, now with a Coupled Torsional Potential, *Comput. Phys. Comm*. 2013, **184**, 2032–2033.
[121] J. J. Wu, H. B. Ning, X. F. Xu, W. Ren, Accurate Entropy Calculations for Large Flexible Hydrocarbons using a Multi-Structural 2-Dimensional Torsion Method, *Phys. Chem. Chem. Phys*. 2019, **21**, 10003-10010.
[122] C. He, Y. Chi, P. Zhang, Approximate Reconstruction of Torsional Potential Energy Surface based on Voronoi Tessellation, *Proc. Combust. Inst*. 2021, **38**, 757-766.
[123] J. Zheng, T. Yu, E. Papajak, I. M. Alecu, S. L. Mielke, D. G. Truhlar, Practical Methods for Including Torsional Anharmonicity in Thermochemical Calculations on Complex Molecules: The Internal Coordinate Multi-Structural Approximation, *Phys. Chem. Chem. Phys*. 2010, **13**, 10885-10907.
[124] Q. Meng, L. Zhang, Q. Chen, Y. Chi, P. Zhang, Influence of Torsional Anharmonicity on the Reactions of Methyl Butanoate with Hydroperoxyl Radical, *J. Phys. Chem. A*, 2020, **124**, 8643-8652.
[125] J. Gang, M. J. Pilling, S. H. Robertson, Monte Carlo Calculation of Partition Functions for Straight Chain Alkanes, *Chem. Phys*. 1998, **231**, 183-192.
[126] Y. Georgievskii, S. N. Elliott, K. B. Moore, S. J. Klippenstein, unpublished.
[127] Y. Fang, F. Liu, S. J. Klippenstein, M. I. Lester, Direct Observation of Unimolecular Decay of CH_3CH_2CHOO Criegee Intermediates to OH Radical Products, *J. Chem. Phys*. 2016, **145**, 044312.
[128] V. P. Barber, S. Pandit, A. M. Green, N. Trongsiriwat, P. J. Walsh, S. J. Klippenstein, M. I. Lester, Four-Carbon Criegee Intermediate from Isoprene Ozonolysis: Methyl Vinyl Ketone Oxide Synthesis, Infrared Spectrum, and OH Production, *J. Am. Chem. Soc.* 2018, **140**, 10866-10880.
[129] A. S. Hansen, Y. Qian, C. A. Sojdak, M. C. Kozlowski, V. J. Esposito, J. S. Francisco, S. J. Klippenstein, M. I. Lester, Rapid Allylic 1,6 H-Atom Transfer in an Unsaturated Criegee Intermediate, *J. Am. Chem. Soc*. 2022, **144**, 5945-5955.
[130] L. Vereecken, A. Novelli, D. Taraborrelli, Unimolecular Decay Strongly Limits the Atmospheric Impact of Criegee Intermediates, *Phys. Chem. Chem. Phys*. 2017, **19**, 31599-31612.
[131] S. M. Aschmann, R. Atkinson, Formation Yields of Methyl Vinyl Ketone and Methacrolein from the Gas-Phase Reaction of O_3 with Isoprene, *Environ. Sci. Technol*. 1994, **28**, 1539−1542.

[132] L. Vereecken, A. Novelli, A. Kiendler-Scharr, A. Wahner, Unimolecular and Water Reactions of Oxygenated and Unsaturated Criegee Intermediates under Atmospheric Conditions. *Phys. Chem. Chem. Phys*. 2022, **24**, 6428−6443.
[133] K. H. Moller, E. Praske, L. Xu, J. D. Crounse, P. O. Wennberg, H. G. Kjaergaard, Stereoselectivity in Atmospheric Autooxidation, *J. Phys. Chem. Lett.* 2019, **10**, 6260-6266.
[134] A. Novelli, L. Vereecken, B. Bohn, H.-P. Dorn, G. I. Gkatzelis, A. Hofzumahaus, F. Holland, D. Reimer, F. Rohrer, S. Rosanka, D. Taraborrelli, R. Tillmann, R. Wegener, Z. Yu, A. Kiendler-Scharr, A. Wahner, H. Fuchs, Importance of Isomerization Reactions for OH Radical Regeneration from the Photo-Oxidation of Isoprene Investigated in the Atmospheric Simulation Chamber SAPHIR, *Atmos. Chem. Phys*. 2020, **20**, 3333-3355.
[135] Y. Xia, B. Long, S. R. Lin, C. Teng, J. L. Bao, D. G. Truhlar, Large Pressure Effects Caused by Internal Rotation in the s-cis-syn Acrolein Stabilized Criegee Intermediate at Tropospheric Temperature and Pressure, *J. Am. Chem. Soc*. 2022, **144**, 4828-4838.
[136] A. D. Danilack, C. R. Mulvihill, S. J. Klippenstein, C. Franklin Goldsmith, Diastereomers and Low-Temperature Oxidation, 2021, **125**, 8065-8073.
[137] S. Y. Mohamed, A. C. Davis, M. J. Al Rashidi, S. M. Sarathy, High-Pressure Limite Rate Rules for α-H Isomerization of Hydroperoxyalkyl Radicals, *J. Phys. Chem. A* 2018, **122**, 3626-3639.
[138] K. B. Moore III, S. N. Elliott, A. V. Copan, C. R. Mulvihill, L. Pratali Maffei, S. J. Klippenstein, Automated Construction of Fully Representative Stereochemical Reaction Mechanisms, 2022 Spring Meeting of the Central States Section of the Combustion Institute; paper 1C14.
[139] A. C. Doner, J. Zador, B. Rotavera, Stereoisomer-Dependent Unimolecular Kinetics of 2,4-Dimehtyloxetane Peroxy Radicals, *Faraday Disc.* 2022, in press.
[140] C. F. Goldsmith, L. B. Harding, Y. Georgievskii, J. A. Miller, S. J. Klippenstein, Temperature and Pressure-Dependent Rate Coefficients for the Reaction of Vinyl Radical with Molecular Oxygen, *J. Phys. Chem. A*, 2015, **119**, 7766-7779.
[141] L. B. Harding, S. J. Klippenstein, Roaming Radical Pathways for the Decomposition of Alkanes, *J. Phys. Chem. Lett.* 2010, **1**, 3016-3020.
[142] S. J. Klippenstein, Y. Georgievskii, L. B. Harding, Statistical Theory for the Kinetics and Dynamics of Roaming Reactions, *J. Phys. Chem. A*, 2011, **115**, 14370-14381.
[143] L. B. Harding, S. J. Klippenstein, A. W. Jasper, Separability of Tight and Roaming Pathways to Molecular Decomposition, *J. Phys. Chem. A*, 2012, **116**, 6967-6982.
[144] K. Yadav, R. Pradhan, U. Lourderaj, Influence of Second-Order Saddles on Reaction Mechanisms, *Faraday Disc*. 2022, in press.
[145] C. D. Foley, C. Xie, H. Guo, A. G. Suits, Quantum Resonances and Roaming Dynamics in Formaldehyde Photodissociation, *Faraday Disc*. 2022, in press.
[146] C. A. Taatjes, F. Liu, B. Rotavera, M. Kumar, R. Caravan, D. L. Osborn, W. H. Thompson, M. I. Lester, Hydroxyacetone Production from C_3 Criegee Intermediates, *J. Phys. Chem. A*, 2017, **121**, 16-23.
[147] K. T. Kuwata, L. Luu, A. B. Weberg, K. Huang, A. J. Parsons, L. A. Peebles, N. B. Rackstraw, M. J. Kim, Quantum Chemical and Statistical Rate Theory Studies of the Vinyl Hydroperoxides Formed in trans-2-Butene and 2,3-Dimethyl-2-butene Ozonolysis, *J. Phys. Chem. A*, 2018, **122**, 2485-2502.
[148] T. Liu, M. Zou, M. F. Vansco, S. N. Elliott, C. R. Markus, R. Almeida, K. Au, L. Sheps, D. L. Osborn, C. J. Percival, C. A. Taatjes, S. J. Klippenstein, R. L. Caravan, M. I. Lester, Novel OH Roaming Pathway in the Unimolecular Decay of Alkyl-Substituted Criegee Intermediates, Poster, *Faraday Disc*. Unimolecular Reactions, 2022.
[149] F. A. L. Mauguiere, P. Collins, Z. C. Kramer, B. K. Carpenter, G. S. Ezra, S. C. Farantos, S. Wiggins, Roaming: A Phase Space Perspective, *Annu. Rev. Phys. Chem.* 2017, **68**, 499-524.
[150] M. Pfeifle, Y.-T. Ma, A. W. Jasper, L. B. Harding, W. L. Hase, S. J. Klippenstein, Nascent Energy Distribution of the Criegee Intermediate CH_2OO from Direct Dynamics Calculations of Primary Ozonide Dissociation, *J. Chem. Phys*. 2018, **148**, 174306.
[151] T. L. Nguyen, H. Lee, D. A. Matthews, M. C. McCarthy, J. F. Stanton, Stabilization of the Simplest Criegee Intermediate from the Reaction between Ozone and Ethylene: A High-Level Quantum Chemical and Kinetic Analysis of Ozonolysis*, J. Phys. Chem. A* 2015, **119**, 5524-5533.
[152] M. J. Newland, C. Mouchel-Vallon, R. Valorso, B. Aumont, L. Vereecken, M. E. Jenkin, A. R. Rickard, Estimation of Mechanistic Parameters in the Gas-Phase Reactions of Ozone with Alkenes for Use in Automated Mechanism Construction, *Atmos. Chem. Phys.* 2022, 2015, 6167-6195.
[153] S. Iyer, M. P. Rissanen, R. Vallev, S. Barua, J. E. Krechmer, J. Thornton, M. Ehn, T. Kurten, Molecular Mechanism for Rapid Autooxidation in α-Pinene Autooxidation, *Nat. Comm.* 2021, **12**, 878.

[154] A. Stagni, A. Cuoci, A. Frassoldati, T. Faravelli, E. Ranzi, Lumping and Reduction of Detailed Kinetic Schemes: An Effective Coupling, *Ind. Eng. Chem. Res*. 2014, **53**, 9004-9016.
[155] N. J. Labbe, R. Sivaramakrishnan, C. F. Goldsmith, Y. Georgievskii, J. A. Miller, S. J. Klippenstein, Weakly Bound Free Radicals in Combustion: "Prompt" Dissociation of Formyl Radicals and its Effect on Laminar Flame Speeds, *J. Phys. Chem. Lett*. 2016, **7**, 85-89.
[156] C. F. Goldsmith, M. P. Burke, Y. Georgievskii, S. J. Klippenstein, Effect of Non-Thermal Product Energy Distributions on Ketohydroperoxide Decomposition, *Proc. Combust. Inst*. 2015, **35**, 283-290.
[157] C. R. Mulvihill, A. D. Danilack, C. F. Goldsmith, M. Demireva, L Sheps, Y. Georgievskii, S. N. Elliott, S. J. Klippenstein, Non-Boltzmann Effects in Chain Branching and Pathway Branching for Diethyl Ether Oxidation, *Energy Fuels*, 2021, **35**, 17890-17908.
[158] J. A. Miller, S. J. Klippenstein, Some Observations Concerning Detailed Balance in Association/Dissociation Reactions, *J. Phys. Chem. A*, 2004, **108**, 8296-8306.
[159] A. D. Danilack, C. F. Goldsmith, A Statistical Model for the Product Energy Distribution in Reactions Leading to Prompt Dissociation, *Proc. Combust. Inst*. 2021, **38**, 507-514.
[160] H. Guo, B. Jiang, The Sudden Vector Projection Model for Reactivity: Mode Specificity and Bond Selectivity Made Simple, *Acc. Chem. Res*. 2014, **47**, 3679-3685.
[161] L. Pratali Maffei, S. J. Klippenstein, work in progress.
[162] L. Lei, M. P. Burke, An Extended Methodology for Automated Calculations of Non-Boltzmann Kinetic Sequences: H + C_2H_2 + X and Combustion Impact, *Proc. Combust. Inst*. 2021, **38**, 661-669.
[163] R. J Shannon, S. H. Robertson, M. A. Blitz, P. W. Seakins, Bimolecular Reactions of Activated Species: An Analysis of Problematic HC(O)C(O) Chemistry, *Chem. Phys. Lett*. 2016, **661**, 58-64.
[164] N. J. B. Green, S. H. Robertson, General Master Equation Formulation of a Reversible Dissociation/Association Reaction, *Chem. Phys. Lett*. 2014, **605-606**, 44-46.
[165] A. W. Jasper, R. Sivaramakrishnan, S. J. Klippenstein, Nonthermal Rate Constants for CH_4^* +X $\rightarrow$ CH_3 + HX, X = H, O, OH, and O_2, *J. Chem. Phys*. 2019, **150**, 114112.
[166] Y. Tao, A. W. Jasper, Y. Georgievskii, S. J. Klippenstein, R. Sivaramakrishnan, Termolecular Chemistry Facilitated by Radical-Radical Recombinations and its Impact on Flame Speed Predictions, *Proc. Combust. Inst*. 2021, **38**, 515-522.
[167] M. P. Burke, S. J. Klippenstein, Ephemeral Collision Complexes Mediate Chemically Termolecular Transformations that Affect System Chemistry, *Nat. Chem*. 2017, **9**, 1078-1082.
[168] J. M. C. Plane, S. H. Robertson, Master Equation Modelling of Non-Equilibrium Chemistry in Stellar Outflows, *Faraday Disc*. 2022, in press.
[169] M. P. Burke, Q. Meng, C. Sabaitis, Dissociation-Induced Depletion of High-Energy Reactant Molecules as a Mechanism for Pressure-Dependent Rate Constants for Bimolecular Reactions, *Faraday Disc*., 2022, in press.
[170] R. M. Zhang, W. Chen, D. G. Truhlar, X. Xu, Master Equation Study of Hydrogen Abstraction from HCHO by OH via a Chemically Activated Intermediate, *Faraday Disc.* 2022, in press.
[171] C. Sleiman, S. Gonzalez, S. J. Klippenstein, D. Tabli, G. El Dib, A. Canosa, Pressure Dependent Low Temperature Kinetics for CN + CH_3CN: Competition Between Chemical Reaction and van der Waals Complex Formation, *Phys. Chem. Chem. Phys.* 2016, **18**, 15118- 15132.
[172] T. L. Nguyen, J. F. Stanton, Pressure-Dependent Rate Constant Caused by Tunneling Effects: OH + HNO_3 as an Example, *J. Phys. Chem. Lett.* 2020, **11**, 3712-3717.
[173] J. F. Muller, Z. Liu, V. S. Nguyen, T. Stavrakou, J. N. Harvey, J. Peeters, The Reaction of Methyl Peroxy and Hydroxyl Radicals as a Major Source of Atmospheric Methanol, *Nat. Comm*. 2016, **7**, 13213.
[174] R. L. Caravan, M. A. H. Khan, J. Zador, L. Sheps, I. Antonov, B. Rotavera, K. Ramsesha, K. Au, M.-W. Chen, D. Rosch, D. L. Osborn, C. Fittschen, C. Schoemaecker, M. Duncianu, A. Grira, S. Dusanter, A. Tomas, C. J. Percival, D. E. Shallcross, The Reaction of Hydroxyl and Methylperoxy Radicals is Not a Source of Atmospheric Methanol, *Nat. Comm*. 2018, **9**, 4343.
[175] E. Assaf, C. Schoemaecker, L. Vereecken, C. Fittschen, Experimental and Theoretical Investigation of the Reaction of RO2 Radicals with OH Radicals: Dependence of the HO_2 Yield on the Size of the Alkyl Group, *Int. J. Chem. Kinet*. 2018, **50**, 670-680.
[176] F. Zhang, C. Huang, Pressure-Dependent Kinetics of the Reaction between CH_3OO and OH Focusing on the Product Yield of Methyltrioxide (CH_3OOOH), *J. Phys. Chem. Lett*. 2019, **10**, 3598-3603.
[177] C. Yan, L. N. Krasnoperov, Pressure-Dependent Kinetics of the Reaction Between CH_3O_2 and OH: TRIOX Formation, *J. Phys. Chem. A*, 2019, **123**, 8349-8357.

[178] C. Fittschen. M. Al Ajami, S. Batut, V. Ferraci, S. Archer-Nicholls, A. T. Archibald, C. Schoemaecker, ROOOH: A Missing Piece of the Puzzle for OH Measurements in Low-NO Environments, *Atmos. Chem. Phys*. 2019, **19**, 349-362.
[179] S. J. Klippenstein, R. Sivaramakrishnan, U. Burke, K. P. Somers, H. J. Curran, L. Cai, H. Pitsch, M. Pelucchi, T. Faravelli, P. Glarborg, $HO_2 + HO_2$: High Level Theory and the Role of Singlet Channels, *Combust. Flame*, 2022, **236**, 111975.
[180] K. T. Kuwata, M. P. DeVault, D. J. Claypool, Improved Computational Modeling of the Kinetics of the Acetylperoxy + HO_2 Reaction, *Faraday Disc*. 2022, in press.
[181] G. Ghigo, A. Maranzana, G. Tonachini, Combustion and Atmospheric Oxidation of Hydrocarbons: Theoretical Study of the Methyl Peroxyl Self-Reaction, *J. Chem. Phys*. 2003, **118**, 10575-10583.
[182] R. Lee, G. Gryn'ova, K. U. Ingold, M. L. Coote, Why are sec-Alkylperoxyl Bimolecular Reactions Orders of Magnitude Faster Than the Analagous Reactions of tert-Alkylperoxyls? The Unanticipated Role of Hydrogen Bond Donation, *Phys. Chem. Chem. Phys*. 2016, **18**, 23673-23679
[183] R. R. Valiev, G. Hasan, V.-T. Salo, J. Kubecka, T. Kurten, Intersystem Crossings Drive Atmospheric Gas-Phase Dimer Formation, *J. Phys. Chem. A*, 2019, **123**, 6596-6604.
[184] G. Hasam. V.-T. Salo, R. R. Valiev, J. Kubecka, T. Kurten, Comparing Reaction Routes for ^{3}(RO…OR') Intermediates Formed in Peroxy Radical Self- and Cross-Reactions, *J. Phys. Chem. A*, 2020, **124**, 8305-8320.
[185] C. D. Daub, I. Zakai, R. Valiev, V.-T. Salo, R. B. Gerber, T. Kurten, Energy Transfer, Pre-Reactive Complex Formation and Recombination Reactions During the Collision of Peroxy Radicals, *Phys. Chem. Phys*. 2022, **24**, 10033-10043.
[186] M. E. Jenkin, R. Valorso, B. Aumont, A. R. Rickard, Estimation of Rate Coefficients and Branching Ratios for Reactions of Organic Peroxy Radicals for Use in Automated Mechanism Construction, *Atmos. Chem. Phys*. 2019, **19**, 7691-7717.
[187] G. Sun, S. Han, X. Zheng, Y. Song, Y. Qin, R. Dawes, D. Xie, J. Zhang, H. Guo, Unimolecular Dissociation Dynamics of Electronically Excited HCO($\tilde{A}^2A''$): Rotational Control of Nonadiabatic Decay, *Faraday Disc*. 2022, in press.
[188] A. W. Jasper, Multidimensional Effects in Nonadiabatic Statistical Theories of Spin-Forbidden Kinetics: A Case Study of $^3O + CO \rightarrow CO_2$, *J. Phys. Chem. A*, 2015, **119**, 7339-7351.
[189] A. W. Jasper, C. Zhu, S. Nangia, D. G. Truhlar, Introductory Lecture: Nonadiabatic Effects in Chemical Dynamics, *Faraday Disc*. 2004, **127**, 1-22.
[190] J. Aerssens, F. Vermeire, S. U. Arravindikashan, R. Van de Vivjer, K. M. Van Geem, The Merit of Pressure Dependent Kinetic Modelling in Steam Cracking, *Faraday Disc*. 2022, in press.
[191] J. R. Barker, Energy Transfer in Master Equation Simulations: A New Approach, *Int. J. Chem. Kinet*. 2009, **41**, 748-763.
[192] R. M. Zhang, X. F. Xu, D. G. Truhlar, Energy Dependence of Ensemble-Averaged Energy Transfer Moments and its Effect on Competing Decomposition, *J. Phys. Chem. A*, 2021, **125**, 6303-6313.
[193] A. W. Jasper, J. A. Miller, Theoretical Unimolecular Kinetics for $CH_4 + M = CH_3 + H + M$ in Eight Baths, M = He, Ne, Ar, Kr, H_2, N_2, CO, and CH_4, *J. Phys. Chem. A*, 2011, **115**, 6438-6455.
[194] A. W. Jasper, C. M. Oana, J. A. Miller, "Third-Body" Collision Efficiencies for Combustion Modeling: Hydrocarbons in Atomic and Diatomic Baths, *Proc. Combust. Inst*. 2015, **35**, 197-204.
[195] A. W. Jasper, "Third-Body" Collision Parameters for Hydrocarbons, Alcohols, and Hydroperoxides and an Effective Internal Rotor Approach for Estimating Them, *Int. J. Chem. Kinet*. 2020, **52**, 387-402.
[196] A. W. Jasper, Predicting Third-Body Collision Efficiencies for Water and Other Polyatomic Baths, *Faraday Disc*., 2022, in press.
[197] A. W. Jasper, Microcanonical Rate Constants for Unimolecular Reactions in the Low-Pressure Limit, *J. Phys. Chem. A* 2020, **124**, 1205-1226.
[198] A. Matsugi, Origin of Bath Gas Dependence in Unimolecular Reaction Rates, *J. Phys. Chem. A*, 2019, **123**, 764-770.
[199] A. Matsugi, Modeling Third-Body Effects in the Thermal Decomposition of H_2O_2, *Combust. Flame*, 2021, **225**, 444-452.
[200] H. M. Wang, K. C. Wen, X. Q. You, Q. Mao, K. H. Luo, M. J. Pilling, S. H. Robertson, Energy Transfer in Intermolecular Collisions of Polycyclic Hydrocarbons with Bath Gases He and Ar, *J. Chem. Phys*. 2019, **151**, 044301.
[201] A. W. Jasper, M. J. Davis, Parameterization Strategies for Intermolecular Potentials for Predicting Trajectory-Based Collision Parameters, *J. Phys. Chem. A* 2019, **123**, 3464-3480.

[202] D. R. Moberg, A. W. Jasper, Permutationally Invariant Polynomial Expansions with Unrestricted Complexity. *J. Chem. Theory Comput.* 2021, **17**, 5440-5455.
[203] S. C. Smith, R. C. Gilbert, Angular Momentum Conservation in Unimolecular and Recombination Reactions, *Int. J. Chem. Kinet.* 1988, **20**, 307-329.
[204] J. A. Miller, S. J. Klippenstein, C. Raffy, Solution of Some One- and Two-Dimensional Master Equation Models for Thermal Dissociatoin: The Dissociation of Methane in the Low-Pressure Limit, *J. Phys. Chem. A*, 2002, **106**, 4904-4913.
[205] T. L. Nguyen, J. F. Stanton, A Steady-State Approximation to the Two-Dimensional Master Equation for Chemical Kinetics Calculations, *J. Phys. Chem. A*, 2015, **119**, 7627-7636.
[206] T. L. Nguyen, J. F. Stanton, Three Dimensional Master Equation (3DME) Approach, *J. Phys. Chem. A*, 2018, **122**, 7757-7767.
[207] S. J. Jeffrey, K. E. Gates, S. C. Smith, Full Iterative Solution of the Two-Dimensional Master Equation for Thermal Unimolecular Reactions, *J. Phys. Chem*. 1996, **100**, 7090-7096.
[208] S. H. Robertson, M. J. Pilling, K. E. Gates, S. C. Smith, Application of Inverse Iteration to 2-Dimensional Master Equations, *J. Comput. Chem*. 1997, **18**, 1004-1010.
[209] J. R. Barker, R. E. Weston, Collisional Energy Transfer Probability Densities *P*(*E,J;E',J'*) for Monatomics Colliding with Large Molecules, *J. Phys. Chem. A*, 2010, **114**, 10619-10633.
[210] A. W. Jasper, K. M. Pelzer, J. A. Miller, E. Kamarchik, L. B. Harding, S. J. Klippenstein, Predictive A Priori Pressure-Dependent Kinetics, *Science*, 2014, **346**, 1212-1215.
[211] M. Brouard, M. T. Macpherson, M. J. Pilling, Experimental and RRKM Modeling Study of the CH_3 + H and CH_3 + D Reactions, *J. Phys. Chem*. 1989, **93**, 4047–4059.
[212] M. R. Laskowski, T. J. Michael, H. M. Ogden, A. S. Mullin, Rotational Energy Transfer Kinetics of Optically Centrifuged CO Molecules Investigated Through Transient IR Spectroscopy and Master Equation Simulations, *Faraday Disc*. 2022, in press.
[213] A. Matsugi, Modeling Collisional Transitions in Thermal Unimolecular Reactions: Successive Trajectories and Two-Dimensional Master Equation for Trifluoromethan Decomposition in an Argone Bath, *J. Phys. Chem. A*, 2020, **124**, 6645-6659.
[214] A. Matsugi, Two-Dimensional Master Equation Modeling of Some Multichannel Unimolecular Reactions, *J. Phys. Chem. A*, 2021, **125**, 2532-2545.
[215] T. L. Nguyen, J. F. Stanton, Pragmatic Solution for a Fully E,J-Resolved Master Equation, *J. Phys. Chem. A*, 2020, **124**, 2907-2918.
[216] S. J. Klippenstein, From Theoretical Reaction Dynamics to Chemical Modeling of Combustion, *Proc. Combust. Inst.* 2017, **161**, 77-111.
[217] C. A. Whelan, M. A. Blitz, R. Shannon, L. Onel, J. P. Lockhart, P. W. Seakins, D. Stone, Temperature and Pressure Dependent Kinetics of QOOH Decomposition and Reaction with O_2: Experimental and Theoretical Investigations of QOOH Radicals Derived from Cl + $(CH_3)_3COOH$, *J. Phys. Chem*. A 2019, **123**, 10254–10262.
[218] M. C. Barbet, M. P. Burke, Impact of "Missing" Third-Body Efficiencies on Kinetic Model Predictions of Combustion Properties, *Proc. Combust Inst*. 2021, **38**, 425-432.
[219] L. Lei, M. P. Burke, Dynamically Evaluating Mixture Effects on Multi-Channel Reactions in Flames: A Case Study for the CH_3 + OH Reaction, *Proc. Combust. Inst*. 2021, **38**, 443-440.
[220] L. Lei, M. P. Burke, Mixture Rules and Falloff are now Major Uncertainties in Experimentally Derived Rate Parameters for H + O_2 (+M) <-> HO_2 (+M), *Combust. Flame* 2020, **213**, 467-474.
[221] L. Lei, M. P. Burke, Bath Gas Mixture Effects on Multichannel Reactions: Insights and Representations for Systems beyond Single-Channel Reactions, *J. Phys. Chem. A*, 2019, **123**, 631-649.
[222] L. Lei, M. P. Burke, Evaluating Mixture Rules and Combustion Implications for Multi-Component Pressure Dependence of Allyl + HO_2 Reactions, *Proc. Combust. Inst.* 2019, **37**, 355-362.
[223] M. P. Burke, R. B. Song, Evaluating Mixture Rules for Multi-Component Pressure Dependence: H + O_2 (+M) = HO_2 (+M), *Proc. Combust. Inst.* 2017, **36**, 245-253.
[224] A. W. Jasper, J. A. Miller, Lennard-Jones Parameters for Combustion and Chemical Kinetics Modeling from Full-Dimensional Intermolecular Potentials, *Combust. Flame*, 2014, **161**, 101-110.
[225] A. W. Jasper, E. Kamarchik, J. A. Miller, S. J. Klippenstein, First-Principles Binary Diffusion Coefficients for H, H_2, and Four Normal Alkanes + N_2, *J. Chem. Phys*. 2014, **141**, 124313.
[226] N. J. Brown, L. A. J. Bastien, P. N. Price, Transport Properties for Combustion Modeling, *Prog. Energy Combust. Sci*. 2011, **37**, 565-582.

[227] A. W. Jasper, J. A. Miller, K. B. Moore III, 1DMIN: One-Dimensional Minimizations. A code for predicting Lennard–Jones parameters from ab initio full-dimensional intermolecular potentials, 2018, https://github.com/Auto-Mech/onedmin/.
[228] X. You, Y. Li, H. Mo, Y. Gui, Theoretical Studies on Lennard-Jones Parameters of Benzene and Polycyclic Aromatics Hydrocarbons, *Faraday Disc.* 2022, in press.
[229] R. M. Zhang, X. F. Xu, D. G. Truhlar, Low-Pressure Limit of Competitive Unimolecular Reactions, *J. Am. Chem. Soc.* 2020, **142**, 16064-16071.
[230] T. M. Pazdera, J. Wenz, M. Olzmann, The Unimolecular Decomposition of Dimethoxymethane: Channel Switching as a Function of Temperature and Pressure, *Faraday Disc*. 2022, in press.
[231] L. Xing, S. Li, Z. Wang, B. Yang, S. J. Klippenstein, F. Zhang, Global Uncertainty Analysis for RRKM/Master Equation Based Kinetic Predictions: A Case Study of Ethanol Decomposition, *Combust. Flame*, 2015, **162**, 3427-3436.
[232] J. A. Miller, S. J. Klippenstein, Determining Phenomenological Rate Coefficients from a Time-Dependent, Multiple-Well Master Equation: "Species Reduction at High Temperatures", *Phys. Chem. Chem. Phys*. 2013, **15**, 4744-4753.
[233] L. Pratali Maffei, M. Pelucchi, C. Cavallotti, A. Bertolino, T. Faravelli, Master Equation Lumping for Multi-Well Potential Energy Surfaces: A Bridge Between Ab Initio Based Rate Constant Calculations and Large Kinetic Mechanisms, *Chem. Eng. J*. 2021, **422**, 129954.
[234] N. J. B. Green, Z. A. Bhatti, Steady-State Master Equation Methods, *Phys. Chem. Chem. Phys.* 2007, **9**, 4275-4290.
[235] J. W. Allen, C. F. Goldsmith, W. H. Green, Automatic Estimation of Pressure-Dependent Rate Coefficients, *Phys. Chem. Chem. Phys*. 2012, **14**, 1131-1155.
[236] A. Y. Chang, J. W. Bozzelli, A. M. Dean, Kinetic Analysis of Complex Chemical Activation and Unimolecular Dissociation Reactions using QRRK Theory and the Modified Strong Collision Approximation, *Zeit. Phys. Chem.* 2000, **214**, 1533-1568.
[237] J. R. Barker, Multiple-Well, Multiple-Path Unimolecular Reaction Systems. I. MultiWell Computer Program Suite, *Int. J. Chem. Kinet*. 2001, **33**, 232-245.
[238] A. M. Mebel, M. Frenklach, Cleavage of an Aromatic Ring and Radical Migration, *Faraday Disc*. 2022, in press.
[239] C. Cavallotti, Automation of Chemical Kinetics: Status and Challenges, *Proc. Combust. Inst*. 2022, **39**, in press.
[240] J. P. Unsleber, M. Reiher, The Exploration of Chemical Reaction Networks, *Ann. Rev. Phys. Chem*. 2020, **71**, 121-42.
[241] S. Maeda, T. Taketsugu, K. Morokuma, Exploring Transition State Structures for Intramolecular Pathways by the Artificial Force Induced Reaction Method, *J. Comput. Chem*. 2014, **35**, 166-173.
[242] R. Van de Vivjer, J. Zador, KinBot: Automated Stationary Point Search on Potential Energy Surfaces, *Comp. Phys. Comm*. 2020, **248**, 106947.
[243] P. M. Zimmerman, Single-Ended Transition State Finding with the Growing String Method, *J. Comput. Chem.* 2015, **36**, 601-611.
[244] Zimmerman Group, Molecular GSM; https://github.com/ZimmermanGroup/molecularGSM.
[245] M. Dontgen, M. D. Przybylski-Freund, L. C. Kroger, W. A. Kopp, A. E. Ismail, K. Leonhard, Automated Discovery of Reaction Pathways, Rate Constants, and Transition States Using Reactive Molecular Dynamics Simulations, *J. Chem. Theory Comput.* 2015, **11**, 2517-2524.
[246] L. Krep, I. S. Roy, W. Kopp, F. Schmalz, C. Huang, K. Leonhard, Efficient Reaction Space Exploration with ChemTraYzer-TAD, *J. Chem. Inf. Modeling*, 2022, **62**, 1-13.
[247] E. Martinez-Nunez, G. L. Barnes, D. R. Glowacki, S. Kopec, D. Pelaez, A. Rodriguez, R. Rodriguez-Fernandez, R. J. Shannon, J. J. P. Stewart, P. G. Tahoces, S. A. Vazquez, AutoMeKin2021: An Open Source Program for Reaction Discovery, *J. Comput. Chem*. 2021, **42**, 2036-2048.
[248] C. A. Grambow, A. Jamal, Y. P. Li, W. H. Green, J. Zador, Y. V. Suleimanov, Unimolecular Reaction Pathways of a γ-Ketohydroperoxide from Combined Application of Automated Reaction Discovery Methods, J. *Am. Chem. Soc*. 2018, **140**, 1035-1048.
[249] S. Madea, Y. Harabuchi, On Benchmarking of Automated Methods for Performing Exhaustive Reaction Path Search, *J. Chem. Theory Comput*. 2019, **15**, 2111-2115.
[250] J. Zheng, J. L. Bao, S. Zhang, J. C. Corchado, R. Meana-Pañeda, Y.-Y. Chuang, E. L. Coitiño, B. A. Ellingson, D. G. Truhlar, *Gaussrate 17* (University of Minnesota, Minneapolis, MN, 2017); https://comp.chem.umn.edu/gaussrate/
[251] P. L. Bhoorasigh, B. L. Slakman, F. S. Khanshan, J. Y. Cain, R. H. West, Automated Transition State Theory Calculations for High-Throughput Kinetics, *J. Phys. Chem. A*, 2017, **121**, 6896-6904

[252] C. Cavallotti, M. Pelucchi, Y. Georgievskii, S. J. Klippenstein, EStokTP: Electronic Structure to Temperature- and Pressure-Dependent Rate Constants – A Code for Automatically Predicting the Thermal Kinetics of Reactions, *J. Chem. Theory Comput.* 2019, **15**, 1122-1145.
[253] S. N. Elliott, K. B. Moore III, A. V. Copan, M. Keceli, C. Cavallotti, Y. Georgievskii, H. F. Schaefer III, S. J. Klippenstein, Automated Theoretical Chemical Kinetics: Predicting the Kinetics for the Initial Stages of Pyrolysis, *Proc. Combust. Inst.* 2021, **38**, 375-384.
[254] D. P. Zaleski, R. Sivaramakrishnan, H. R. Weller, N. A. Seifert, D. H. Bross, B. Ruscic, K. B. Moore III, S. N. Elliott, A. V. Copan, L. B. Harding, S. J. Klippenstein, R. W. Field, K. Prozument, Substitution Reactions in the Pyrolysis of Acetone Revealed Through a Modeling, Experiment, Theory Paradigm, *J. Am. Chem. Soc.* 2021, **143**, 3124-3142.
[255] A. G. Dana, M. S. Johnson, J. W. Allen, S. Sharma, S. Raman, M. Liu, C. W. Gao, C. A. Grambow, M. J. Goldman, D. S. Ranasinghe, R. J. Gillis, A. M. Payne, Y.-P. Li, E. E. Dames, Z. J. Buras, N. M. Vandewiele, N. W. Yee, S. S. Merchant, B. Buesser, C. A. Class, C. F. Goldsmith, R. H. West, W. H. Green, Automated Reaction Kinetics and Network Exploration (Arkane), 2022, https://github.com/ReactionMechanismGenerator/RMG-Py.